TAMPEREEN TEKNILLINEN YLIOPISTO
TAMPERE UNIVERSITY OF TECHNOLOGY

Marja Rissanen

Wet Spinning of Polylactide Stereo Copolymer Multifilaments

Julkaisu 887 • Publication 887

Tampere 2010

Tampereen teknillinen yliopisto. Julkaisu 887
Tampere University of Technology. Publication 887

Marja Rissanen

Wet Spinning of Polylactide Stereo Copolymer Multifilaments

Thesis for the degree of Doctor of Technology to be presented with due permission for public examination and criticism in Festia Building, Auditorium Pieni Sali 1, at Tampere University of Technology, on the 4th of June 2010, at 12 noon.

Tampereen teknillinen yliopisto - Tampere University of Technology
Tampere 2010

ISBN 978-952-15-2360-1 (printed)
ISBN 978-952-15-2416-5 (PDF)
ISSN 1459-2045

ABSTRACT

Polylactide is biodegradable and bioresorbable polymer which is used in fibers, packaging, and medical applications. The main method to manufacture polylactide fibers is melt spinning. In this process a molten polymer is extruded through a spinneret and polymer jets are cooled and winded. During the heating the polymer is exposed to a high temperature which can cause a thermo-oxidative degradation of the polymer, and it can be observed in a decrease of molar mass. Furthermore, heat-sensitive additives cannot be added to the polymer melt. During wet spinning polymer is not exposed to the elevated temperature. In this process the polymer solution is extruded through the spinneret, and the filaments are coagulated in a spin bath containing non-solvent of the polymer.

The aim of this thesis was to describe the manufacturing process of wet-spun polylactide stereo copolymer multifilament fibers and to study the filament properties. The first step was to study the solubility and phase separation properties of polylactide stereo copolymers. According to this study dichloromethane was chosen for polymer solvent and methanol and ethanol for non-solvents to the further wet spinning studies. The effect of spin drawing, hot drawing and protein-loading on the physical and mechanical properties, and hydrolytic degradation was examined.

The filaments had a skin-core structure which is typical for wet-spun filaments. This structure was more distinct with poly(L/D-lactide), L to D ratio 96/4, filaments, and the phase separation ability of this polymer was observed faster than that of poly(L/DL-lactide), L to DL ratio 70/30. The increase of the spin draw ratio up to 7.0 improved the tensile strength of filaments. The further increase of the spin draw ratio decreased the tensile strength due to the overstretching of polymer chains. Hot drawing was performed just above the glass transition temperature of polymers. It increased also the tensile strength of the filaments, but hydrolytic degradation rate became slower because of the increased degree of crystallinity. The protein-loaded filaments were more porous than the unloaded filaments due to the probe sonication of the polymer solution. The mechanical properties were also lower compared to the unloaded filaments.

Despite the mechanical properties of the wet-spun filaments were not as high as the normal textile fibers, they are sufficient, for example, for the non-woven production. The diameter of the wet-spun filaments was as lowest about 10 μm, and this size is suitable, for example, for tissue engineering. The described manufacturing method is practical for the small-scale filament production.

PREFACE

I wish to express my gratitude to Professor Pertti Nousiainen for supervision of my thesis. The official examiners of this thesis, Professor Piet J. Lemstra and Professor Jukka Seppälä, are gratefully acknowledged for useful suggestions and remarks.

I wish to thank my co-authors of the papers, both at Tampere University of Technology and at National University of Ireland. I want to thank Arja Puolakka, Ville Ellä, Niina Ahola, Professor Minna Kellomäki, Terttu Hukka, Aaron Torny, and Yury Rochev for the help of preparing the papers. I also want to thank Keijo Granholm for installing the spinning equipment and Eira Lehtinen for the help with the *in vitro* tests.

This work was carried out in the Department of Materials Science at Tampere University of Technology during the years 2005 - 2009. I am grateful to all the staff at the Department of Materials Science, Laboratory of Fiber Materials Science, for the pleasant work atmosphere.

I acknowledge the financial support provided by European Commission within the Sixth Framework Programme (NMP-CT-2005-013633) and Tampere City Science Foundation.

Tampere, April 2010
Marja Rissanen

CONTENTS

LIST OF ORIGINAL PUBLICATIONS

This thesis is based on the following original publications, presented as Papers I to IV:

I. Rissanen, M., Puolakka, A., Nousiainen, P., Kellomäki, M. & Ellä, V. 2008. Solubility and Phase Separation of Poly(L,D-lactide) Copolymers. Journal of Applied Polymer Science, 110, pp. 2399-2404.

II. Rissanen, M., Puolakka, A., Hukka, T., Ellä, V., Nousiainen, P. & Kellomäki, M. 2009. Effect of Process Parameters on Properties of Wet-Spun Poly(L,D-lactide) Copolymer Multifilament Fibers. Journal of Applied Polymer Science, 113, pp. 2683-3692.

III. Rissanen, M., Puolakka, A., Hukka, T., Ellä, V., Kellomäki, M. & Nousiainen, P. 2010. Effect of Hot Drawing on Properties of Wet-Spun Poly(L,D-lactide) Copolymer Multifilament Fibers. Journal of Applied Polymer Science, 115, pp. 608-615.

IV. Rissanen, M., Puolakka, A., Ahola, N., Torny, A., Rochev, Y., Kellomäki, M. & Nousiainen, P. 2010. Effect of Protein-Loading on Properties of Wet-Spun Poly(L,D-lactide) Multifilament Fibers. Journal of Applied Polymer Science, 116, pp. 2174-2180.

AUTHOR'S CONTRIBUTION

The author planned and performed the experimental tests, interpreted the results and was responsible for the preparation of the original papers. The co-authors commented the results, revised the publications, and made suggestions for the improvement of the manuscript. The need of protein-loading filaments for tissue engineering scaffolds was given by the co-authors from NCBES, Ireland.

LIST OF SYMBOLS AND ABBREVIATIONS

Symbols

α	concentration of spin dope
A_0	original cross sectional area
a	correction factor
δ_d	dispersion component of solubility parameter
δ_h	hydrogen component of solubility parameter
δ_p	polar component of solubility parameter
δ_{total}	total solubility parameter
ε	engineering strain
F	force
f	natural frequency of transverse vibration
ΔG_M	free energy of mixing
H	enthalpy
ΔH_c	crystallization enthalpy
ΔH_m	melting enthalpy
ΔH_M	mixing enthalpy
l	length
l_0	original length of specimen
Δl	change in length
M_n	number average molar mass
M_v	viscosity average molar mass
M_w	weight average molar mass
m	mass per unit length
n	number of spinneret orifices
ρ	density of spin dope
Q	capacity of pump
σ	engineering stress
ΔS_M	entropy change in mixing process
T	absolute temperature
T	tension
T_{cc}	peak temperature of cold-crystallization

T_g	glass transition temperature
T_m	melting temperature
Ti	titer
v	take-up velocity
χ	Flory's or Flory-Huggins χ parameter
X	initial degree of crystallinity
X_c	degree of crystallinity
X_{cc}	degree of cold-crystallinity

Abbreviations

BSA	bovine serum albumin
CF	ciprofloxacin
CL_{ns}	cloud point of non-solvent
DSC	differential scanning calorimeter
Et-OH	ethanol
HDR	hot draw ratio
HSP	Hansen Solubility Parameter
IV	inherent viscosity
L	long coagulation time
LOI	Limited Oxygen Index
Met-OH	methanol
PD	polydispersity
P(D)LA	poly(D-lactide)
PDLGA	poly(DL-lactide-co-glycolide)
P(L)LA	poly(L-lactide)
P(L/D)LA	poly(L/D-lactide), L-lactide/D-lactide copolymer
P(L/DL)LA	poly(L/DL-lactide), L-lactide/DL-lactide copolymer
RH	relative humidity
S	short coagulation time
SDR	spin draw ratio
SEM	scanning electron microscope
SR	self reinforced

1 INTRODUCTION

The total world production of textile fibers was about 69 million tons in the year 2008 [CIRFS 2009, p. 19]. It was about 5 million tons less than in the year 2007 when the maximum textile fiber production was reached. However, from the year 2002 to the year 2007 the increase of the textile fiber production has been about 30%. The increase of the total production can be explained by the increase of the synthetic fiber production, especially by the increase of the polyester production, and by the application of biotechnology in the cotton growing helping to improve a yield per hectare. In 2008 the total synthetic fiber production was about 41 million tons, from which the production of polyester was about three quarters. The raw cotton production was about 23 million tons in the year 2008.

The raw materials of polyester are based on non-renewable crude oil, whereas polylactide fiber, which is also a synthetic fiber, is possible to produce from renewable agricultural crops. The main resource of polylactide is starch from corn, but it can be prepared from wheat, sugar beets of other grown biomass materials. The production of polylactide polymer uses less fossil fuel and emits less greenhouse gases than traditional petroleum based polymers [Vink *et al.* 2003]. Polylactide fiber has two major properties: biodegradability and biocompatibility. Its biodegradability, and its possibility to produce from annually renewable resources makes it ecologically and environmentally sustainable fiber polymer. Its biocompatibility makes it suitable for medical end-uses.

The end-uses of polylactide fibers are, for example, apparel, furnishing, carpets, agricultural and geotextiles, wipes, hygiene products and fibrefill [Vink *et al.* 2004]. It is possible to use as 100% polylactide or it can be blended with other textile fibers. Polylactide fiber is suitable for outdoor end-uses, because it has high resistance to ultraviolet light. Its biodegradability gives benefits especially in the use of disposable products compared to the conventional petroleum based fibers.

As mentioned, polylactide is widely used in medical applications because of its biocompatibility and bioresorbability. The medical end-uses are, for example, sutures,

bone fixation devices, and tissue engineering scaffolds [Eppley 2003; Maurus & Kaeding 2004]. The bioresorbable bone fixation devices do not need the second surgery to remove the fixation device compared to the biostable devices. Tissue engineering stimulates an organ-specific environment to allow cell development *in vitro*, and the scaffold supports cell attachment and gives the architecture to formation of native tissue.

The objective of this thesis is to describe the fabrication of multifilaments using the wet spinning process from the medical grade polylactide stereo copolymers, and to characterize the unmodified and modified wet-spun filaments. The target was to fabricate thin, bendable fibers which were able to use in the textile manufacturing processes. The fibers were supposed to be mouldable for 3D structures. The medical grade polylactide was used because the end-use of fibers was scaffold in tissue engineering. The mechanical strength of fibers in tissue engineering is not as important as in sutures or bone fixation materials.

This thesis is based on four scientific papers published in refereed journals. It also contains a summary which consist a literature review and an experimental section. The literature review, Chapter 2, reports the preparation of polylactide polymer and the different spinning methods of polylactide fibers. The experimental part consists of four papers which are included as annexes to this summary as Papers I - IV. Chapter 3 summarizes the materials and the experimental methods used in this thesis. In Chapter 4 are the main results from papers I – IV and the discussion about the results. The conclusions are in Chapter 5.

2 SPINNING OF POLYLACTIDE AND ITS STEREO COPOLYMERS

In this chapter a brief introduction of the raw materials and the polymerization of polylactide and its stereo copolymers is given. After that the spinning methods of the polylactide fibers are presented, including melt spinning, dry spinning, wet spinning, dry wet spinning, and finally shortly electrospinning. The wet spinning method is described in detail because the experimental part is based on this spinning method. The electrospinning method and the studies of nano-scale fibers are not covered precisely because this work focuses on the manufacturing of normal-scale filaments.

2.1 POLYLACTIDE AND ITS STEREO COPOLYMERS

Polylactide is synthetic aliphatic polyester which basic constitutional unit is lactic acid. Lactic acid can be manufactured by chemical synthesis or by carbohydrate fermentation which is the main method. Lactic acid (2-hydroxypropionic acid) ($C_3H_6O_3$) exists in two optically active configurations, the L(+) and D(-) isomers, as shown in Figure 1. Both L and D isomers can be produced by bacterial fermentation of carbohydrates, whereas mammalian systems produce only L isomer. Fermentation can be performed in batch, continuous, or cell recycle reactors [Auras *et al.* 2004]. The produced lactic acid can be purified via distillation.

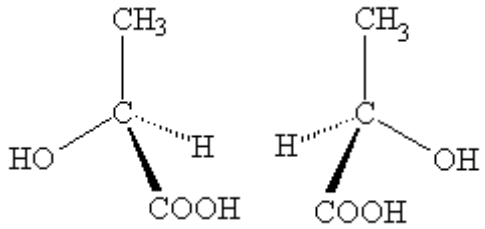

(a) (b)

Figure 1 Chemical structure of lactic acid stereoisomers: (a) L-lactic acid and (b) D-lactic adic.

High molar mass polylactide can be produced by direct condensation polymerization, azeotropic dehydrative condensation, and indirect ring opening polymerization through a

dimer of lactic acid which is the main production method. Lactide dimer (3,6-dimethyl-1,4-dioxane-2,5-dione) is a cyclic diester of lactic acid which can consist of two L-lactic acid molecules, two D-lactic acid molecules, or a L- and a D-lactic acid molecule. Respectively, they can be called L-lactide, D-lactide, and LD-lactide or *meso*-lactide, and they are shown in Figure 2. The equimolar mixture of L-lactide and D-lactide can be called a rasemic lactide (*rac*-lactide) or DL-lactide. Ring opening polymerization is performed in a high temperature and catalyzed by stannous compounds [Perrin & English 1997].

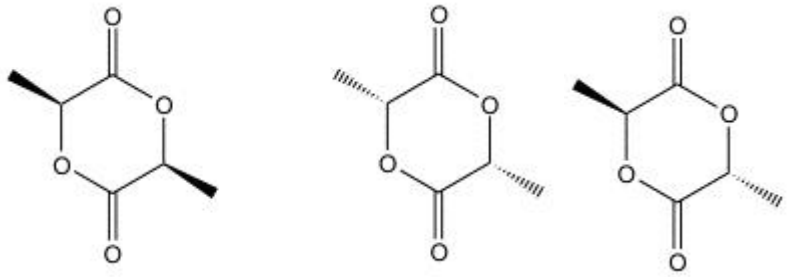

(a) (b) (c)

Figure 2 Stereoisomers of lactide: (a) L-lactide, (b) D-lactide, and (c) *meso*-lactide [Johnson *et al.* 2003].

The properties of polylactide depend on its molecular characteristics and the presence of ordered structure. For example, the properties can be controlled by the copolymerization of different stereoforms.

Enantiomerically pure polylactide is an isotactic polymer which can form crystals, and it is partially crystalline polymer (45-70%) [Huang 2005]. Whereas polymers formed from *meso*- and rasemic lactides are atactic polymers, and they cannot crystallize, and therefore they are amorphous. Stereo copolymers can form crystals, when the amount of L-lactide is more than 87.5 mol-% [Kellomäki *et al.* 2003, Huang 2005], and otherwise they are amorphous.

Depending on the conditions polylactide can crystallize in three forms (α, β and γ). The most common α-form is transformed to the β-form by high draw ratios and high draw temperatures [Eling *et al.* 1982]. The γ-form is formed by the epitaxial crystallization [Cartier *et al.* 2000].

In addition of homocrystals, polylactide can form stereocomplex crystals if both L- and D-stereoforms are present in the system. Stereocomplexation can occur in solution, in a solid state from the melt, during polymerization, or during hydrolytic degradation [Tsuji 2005]. The equimolar mixing of both stereoforms is the most favourable for forming stereocomplex crystals [Tsuji *et al.* 1991].

A melting temperature (T_m) depends on the crystalline structure of polylactide. Typically it ranges from 130 to 180°C. The α-form has the T_m of 185°C, whereas β-form melts at 175°C [Hoogsten *et al.* 1990]. The T_m can be decreased from 20 to 50°C by the addition of D-lactide to the polymer structure. A glass transition temperature (T_g) of enantiomerically pure polylactide is about 55°C [Södergård & Stolt 2002]. Although the T_m is rather low, polylactide has low flammability and smoke generation. The Limited Oxygen Index (LOI) –value is 26 [Linneman *et al.* 2003]. Textile is flame retardant, when the LOI-value is more than 26. For example, LOI-value of commercial textile grade polyester is in the range of 20 - 21 and that of cotton 18 – 19. [Schindler & Hauser 2004]

The sterocomplexation of polylactide effects on its thermal properties. The reported T_m values of stereocomplexed polylactide have been in the range from 220 to 230°C, and the T_g values between 65 and 72°C [Tsuji 2005]. The better thermal properties enable the more extensive application areas of polylactide fiber. For example, in the apparel industry the higher dyeing or ironing temperatures are possible without the fiber damage. Also the automotive industry can use more heat-resistant polylactide fibers for upholstery or composite reinforcing.

The density of amorphous poly(L-lactide) [P(L)LA] is 1.25 g/cm^3 and that of crystalline P(L)LA is 1.29 g/cm^3, but the density values of 1.36 g/cm^3 have been reported for solid polylactide [Auras *et al.* 2004].

The moisture regain of polylactide is very low, only 0.4 – 0.6 % at 65 % RH, 25ºC [Linneman *et al.* 2003]. Because polylactide adsorbs only a limited amount of water, it causes problems in their electrostatic behaviour. This can create, for example, fiber entanglements in the textile manufacturing. However, the low water adsorption increases the moisture wicking property, and this offers benefits in the end-uses of filaments.

Polylactide degrades primarily by hydrolysis, and the degradation occurs in two stages. The first stage is a random non-enzymatic chain scission of the ester groups, and it leads to a reduction in molar mass. Acids or bases accelerate the degradation, and also temperature and moisture levels have effect on it. The cleavage of the ester linkages is autocatalyzed by the carboxylic acid end groups. The chain scission occurs mainly in the amorphous area of polylactide. In the second stage the low molar mass polylactide can diffuse out from the bulk polymer, and they are metabolized by microorganism to yield carbon dioxide and water. Enzymes affect on low molar mass oligomers because they are large molecules and cannot diffuse through crystalline regions. Many factors, such as particle size and shape, temperature, moisture, crystallinity, % isomer, residual lactic acid concentration, molar mass, molar mass distribution, water diffusion and metal impurities from the catalyst, affect on the degradation rate of polylactide. [Auras *et al.* 2004]

The stereocomplexation of polylactide affects its degradation properties. Tsuji [2000] has observed that stereocomplex polylactide has higher resistance to hydrolysis than homo-crystal P(L)LA or poly(D-lactide) [P(D)LA]. Sterocomplexated polylactide has the strong interaction between L- and D-lactide unit sequences which decreases the diffusion of water molecules into the amorphous area.

2.2 SPINNING OF POLYLACTIDE

The fiber spinning methods can be classified into two main categories: melt spinning and solution spinning. Furthermore, solution spinning can be divided into dry spinning and wet spinning. The combination of dry and wet spinning is dry wet spinning. The novel electrospinning is a drawing method of polymer jets, but it can be considered as a spinning method.

In order to obtain the desired mechanical properties (tensile strength, modulus, and elongation) of the filaments they have to be drawn. The drawing process orientates the polymer molecules into alignment of the long axis of fibers. During the drawing the diameter of the filament decreases and the tensile strength increases. Also the appearance of the filaments changes from opaque to translucent. The parameters affecting on the drawing are polymer material, spinning conditions, drawing temperature, and draw ratio.

The draw ratios reach 1:4.5 for normal tenacity synthetic filaments, 1:7 for high tenacity filaments, and as high as 1:several hundred for gel-spun filaments [Fourne 1999, p. 193]. The optimum drawing temperature for normal tenacity synthetic filaments is around or just below the glass transition temperature and it can be generated by outside heating (heated godets, oven, or water bath) and partly by the inner frictional heat. The heated water bath is normally used in the wet spinning process.

Polylactide filaments can be spun by all the main spinning methods [Gupta *et al.* 2007b]. However, melt spinning is the main production method of polylactide textile fibers [Linnemann *et al.* 2003; Perepelkin 2002]. Cargill has introduced Ingeo™ melt-spun fibers made from NatureWorks™ polylactide in 2003 [Vink *et al.* 2004]. Other commercial polylactide fibres are for example Lactron made by Kanebo of Japan [Yamanaka 1999]. Teijin Fibers Limited has introduced stereocomplex polylactide fiber (Biofront™) which has improved hydrolytic resistance in hot and humid conditions. According to Teijin [2009], Biofront™ fiber has the same hydrolytic resistance as polyethylene terephtalate, and it is suitable, for example, for a car seat fabric.

2.2.1 Melt Spinning

In the melt spinning process polymer is melted, filtered, and extruded through the spinneret. The spinnerets of a diameter between 0.1 – 0.7 mm are commonly used for melt spinning [Fourne 1999, p. 178]. The melt is drawn from the spinneret hole at a melt temperature. In the draw zone the extruded filaments are cooled to the solidification temperature and further to below the glass transition temperature. Finally, the filaments come to the take-up mechanism, and the temperature of the filaments is less than the T_g. The additional drawing happens between the godets. Examples of typical melt-spun filaments are polyester, polyamide, and polypropylene. The schematic drawing of the melt spinning equipment is presented in Figure 3. During melt spinning the polymer is subjected to direct heating, conversion of mechanical energy related to screw speed and torque, and the residence time that can cause a thermo-oxidative degradation indicated by a decrease in molar mass [Wang, Y. *et al.* 2008].

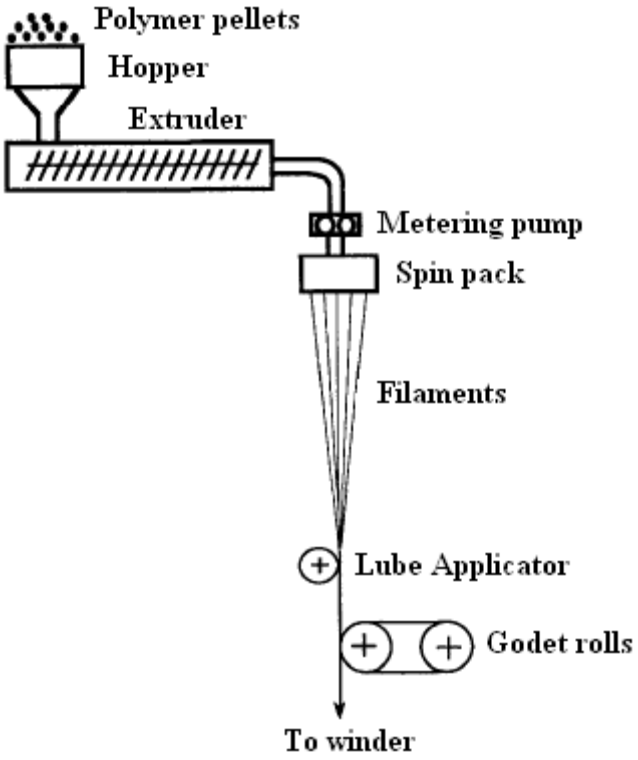

Figure 3 Schematic drawing of melt spinning equipment [Spruiell & Bond 1999].

Many studies have described the melt spinning of P(L)LA, but only few studies have focused on other stereo isomers or stereo copolymes. The studies of polylactide melt spinning can be divided on the studies of low-speed spinning and that of high-speed spinning.

Fambri and co-workers [1997] have melt-spun P(L)LA (M_v = 3.3 x 10^5 g/mol) at extrusion temperature of 240°C and hot-drawn at separate process at 160ºC. The spinning velocities ranged from 1.8 to 20 m/min. The achieved maximum tensile modulus was 9.2 GPa and tensile strength of 0.87 GPa at collection speed of 5 m/min and at the draw ratio of 10. They used low collection speed because it enabled higher draw ratio. The degree of crystallinity of this fiber was about 60 %, and it increased with the increasing draw ratio.

Yuan and co-workers [2001] have melt-spun P(L)LA (M_v = 2.6 – 4.9 x 10^5 g/mol) filaments at extrusion temperature ranging from 200 to 240°C and the spinning speed of 3.2 m/min. The filaments were drawn at 120°C. The maximum tensile modulus was

5.2 GPa and the maximum ultimate strength was 0.54 GPa obtained at an extrusion temperature of 220°C. The degrees of crystallinity of as-spun samples ranged from 42 to 46 %. Hot drawing increased the degree of crystallinity, and it ranged from 50 to 64 %.

Nishimura and co-workers [2005] have melt-spun P(L)LA (M_v = 1.7 x 10^5 g/mol) at the extrusion temperature of 220ºC with the take-up speed of 8 m/min, cooled in the water bath at 45ºC, and finally hot-drawn twice in the water baths at 98ºC. The draw ratios ranged from 1 to 18. The maximum mechanical strength values were obtained at the highest draw ratio. The maximum tensile modulus was 10.7 GPa and tensile strength 0.81 GPa. The degree of crystallinity was between 68 – 71 % depending on the measuring instrument. They explained the increasing mechanical strength by the increasing number of extended chain crystals and tie molecules in the amorphous regions between the crystalline regions.

Cicero and Dorgan [2001] have spun standard fiber grade poly(L/D-lactide) [P(L/D)LA], L/D ratio 98/2, copolymer (M_w = 0.99 x 10^5 g/mol and M_w = 1.1 x 10^5 g/mol) by two-step melt spinning. The spinning speed was about 55 m/min and the filaments were drawn with the second godet. The maximum tensile modulus of the filament was 3.2 GPa and the tensile strength was 0.38 GPa. The degree of crystallinity was about 50 %.

Penning and co-workers [1993] have spun P(L/D)LA copolymer, L/D ratio 85/15, (M = 6.0 x 10^5 g/mol) at 150°C and hot-drawn at 60°C. Tensile strength was 0.19 GPa and modulus about 5 GPa.

Fambri and co-workers [2006] have melt-extruded poly(L/DL-lactide) [P(L/DL)LA] copolymer, L/DL ratio 70/30, at the winding speeds between 5 and 70 m/min. The extrusion temperature was in the range from 120 to 195°C. They made hot drawing at different draw ratios, and the maximum tensile modulus of hot-drawn filament was 4 GPa and tensile strength 0.18 GPa.

Weiler and Gogolewski [1996] have extruded circular rods from P(D)LA (M_v = 2.8 x 10^5 g/mol) and Ferguson and co-workers [1996] from P(L/D)LA (M_v = 1.6 x 10^5 g/mol) and P(L/DL)LA (M_v = 2.1 x 10^5 g/mol). In both studies only the bending strengths have been analyzed.

The high-speed spinning has been utilized in several studies. Solarski and co-workers [2005a] have spun and hot-drawn P(L)LA by one-step method. The final spinning speed was up to 700 m/min, and drawing temperatures ranged from 70 to 120ºC. The maximum modulus was 6.6 GPa and the tensile strength was 0.42 GPa. The optimum hot-drawing temperature was 110°C, and according to the authors, the best molecular orientation has been achieved at this temperature.

Ghosh and Vananthan [2006] have spun P(L)LA at spinning speed of 500 and 1850 m/min. The fibers were drawn and heat setted. The as-spun fibers (1850 m/min) had the degree of crystallinity of 6 %, but drawn and heat setted fibers showed much higher crystallinity (60 %). Thermally induced crystallinity had the biggest influence on the development of fiber crystallinity.

Park and co-workers [2007] have spun P(L)LA (M_w = 1.38 x 10^5 g/mol) at spinning speeds up to 4000 m/min and fibers were heat-setted at 100°C. Heat treatment increased the mechanical strength of fibers, but the increased spinning speed was more effective than heat treatment for enhancing the mechanical strength. The maximum breaking stress was achieved at the spinning speed of 4000 m/min. At this spinning speed the breaking stress value was about 6.5 g/d, and the crystallinity of this specimen was 69 %.

Mezghani and Spruiell [1998] have spun P(L)LA (M_w = 2.1 x 10^5 g/mol) at the spinning speeds up to 5000 m/min, but the maximum mechanical strength was achieved at the spinning speeds between 2000 – 3000 m/min. The spinning temperature was 233°C. The maximum modulus of as-spun filament was 6 GPa and tensile strength 0.39 GPa. The degree of crystallinity was about 42 %.

Schmack and co-workers [1999] have melt-spun a copolymer of L-lactide (92 wt%) and *meso*-lactide (8 wt%) (M_w = 1.6 x 10^5 g/mol), and the spinning speeds were up to 5000 m/min. The maximum break stress was achieved at the spinning speed of 3000 m/min, and it was 0.3 GPa and modulus 4.2 GPa. The drawing at 110°C increased the mechanical strength, and the maximum values were achieved at the draw ratio of 6. The break stress was 0.46 GPa and modulus 6.3 GPa at this draw ratio. They [Schmack *et al.* 2004] have also melt spun various grades of P(L/D)LA. The D-lactide content varied between 1 – 8 % and the viscosity average molar mass ranged from 2.1 x 10^5 to 4.1 x 10^5

g/mol. The spinning speeds were in the range 2000 – 5000 m/min. The maximum mechanical strength values were obtained with polymer having the lowest D-lactide content. The maximum tensile modulus was 6.8 GPa and tensile strength was 0.3 GPa.

Furuhashi and co-workers [2006; 2007] have blended equimolar amount of P(L)LA (M_w = 2.2 x 10^5 g/mol) and P(D)LA (M_w = 2.63 x 10^5 g/mol) to form stereocomplex-type melt-spun fibers. The authors have not mentioned the spinning speed. The extrusion temperature was 230°C. The fibers were drawn up to three times at temperatures between 60 and 120°C. Finally, the fibers were annealed between 170 and 200°C. The maximum tensile modulus of filaments was 9 GPa, and the tensile strength of 0.5 MPa was achieved at the draw temperature of 90°C without annealing. Annealing decreased the mechanical strength values, and the optimum annealing temperature was 190°C. Stereocomplex crystals appeared when the drawing temperature was higher than 100°C. The annealing of the drawn fibers increased also the weight fraction of stereocomplex crystals. The mechanical properties of the stereocomplex-type fibers were lower than that of the homo-crystal type fiber. The authors assumed that it was due to the difficulty in forming the stereocomplex phase.

Takasaki and co-workers [2003] have manufactured stereocomplex-type polylactide fiber, and they used spinning speeds up to 7500 m/min. The stereocomplex crystals were obtained when the take-up velocity was over 4000 m/min. Annealing increased the stereocomplex formation.

2.2.2 Dry Spinning

The solution spinning methods, dry spinning and wet spinning, are usually utilized for polymers that do not melt. In both methods polymer is dissolved into solution with 5 - 40 % concentration of solids, or into gel with 2 - 7 % or 40 - 80 % solids [Fourne 1999, p. 181]. The polymer solution is filtrated, de-gassed, and pumped through the spinneret of diameter of 0.05 - 0.25 mm [Fourne 1999, p. 178]. After this, the methods are separated from each others.

In dry spinning solvent evaporates when the polymer solution exits from the spinneret and the filament solidifies. Finally, similarly as in melt spinning, the filaments come to the take-up mechanisms. The dry spinning equipment is presented in Figure 4. For example, acrylic, modacrylic, elastane, and chlorofibres are typical dry-spun textile fibers.

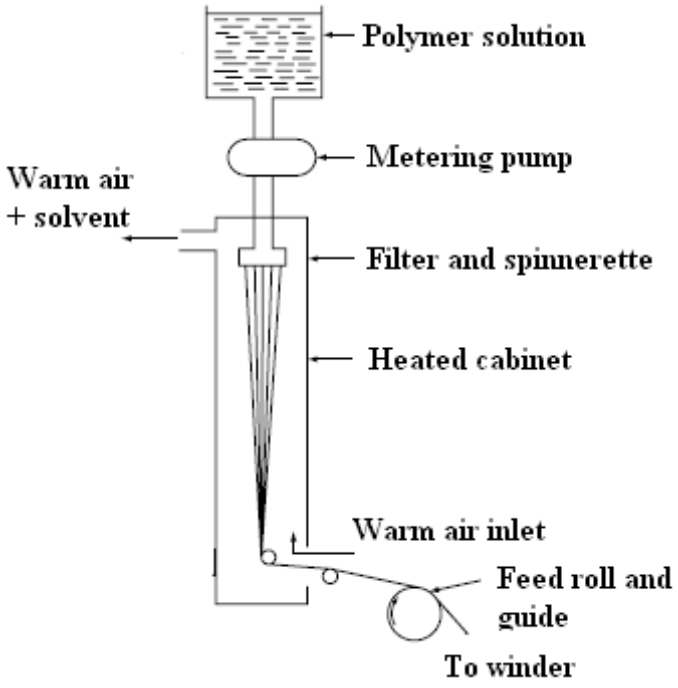

Figure 4 Scematic drawing of dry spinning equipment [LaNieve 2007].

The dry spinning process of the polylactide filaments have been studied widely. The studies have been focused on P(L)LA.

Pennings and co-workers have done very intensive work to study dry spinning of P(L)LA, and they have manufactured very strong monofilaments. They [Eling *et al.* 1982] dissolved P(L)LA (M_v = 3.5 x 10^5 g/mol and M_v = 5.3 x 10^5 g/mol) in toluene and extruded the polymer solution at 110ºC. The filaments were separately hot-drawn at temperatures up to 210ºC. The best drawing temperature was about 190ºC for low molar mass samples and 200ºC for high molar mass samples. The high drawing temperature increased the molecular mobility, and enabled the high draw ratios. The highest tensile strength was 1.0 GPa and modulus 10 GPa. In their other study [Gogolewski & Pennings 1983] P(L)LA was dissolved in dichloromethane or chloroform, extruded, and hot-drawn.

They found that the tensile strength was higher with the high molar mass polymer (M_v = 6.0 x 10^5 g/mol) than with the low molar mass polymer (M_v = 2.0 x 10^5 g/mol), and the tensile strength increased when the polymer concentration in spin dope decreased.

Furthermore, Leenslag and Pennings [1987] have found that the binary solvent system had effect on the tensile strength of P(L)LA (M_v = 9.0 x 10^5 g/mol). Polymer was dissolved in the mixture of chloroform and toluene (40/60) and extruded at 60ºC. The elevated spinning temperature enhanced solvent evaporation. The filaments were also hot-drawn at 204ºC. The highest tensile strength was 2.1 GPa and modulus 16 GPa. A low number of entanglements in the polymer solution and further in the extruded filaments enabled the high draw ratios, and thus high mechanical strength. They [Postema & Pennings 1989] have manufactured even stronger P(L)LA (M_v = 9.1 x 10^5 g/mol) filaments having tensile strength of 2.3 GPa by dry spinning and hot drawing. Hot drawing was taken place at 190ºC, the entrance velocity of drawing was as low as 0.625 cm/min, and the residence time in the oven was about 75 min.

Moreover, they [Postema *et al.* 1990a] have studied the effect of ambient temperature on the tensile strength. The optimal surrounding temperature was 25ºC. The extrusion and winding speed also had effect on the mechanical properties [Postema *et al.* 1990b]. They have studied the spinning speeds ranging from 10 to 182 m/min. The increasing winding speed decreased the tensile strength value, and the lowest winding speed gave the tensile strength of 1.9 GPa.

Most of Pennings' and co-workers studies have been focused on P(L)LA, but they [Penning *et al.* 1993] have also studied dry spinning and hot drawing of P(L/D)LA 95/5 (M = 6.0 x 10^5 g/mol). The maximum tensile strength was 0.95 GPa and modulus 9.2 GPa. The values were higher compared to melt-spun filaments. They have explained the higher values in lower amount of chain entanglements in solution than in melt. If the low entanglement structure was transferred to the solid state in the spinning process, the as-spun filament had a high drawability.

After the intensive work of Penning and co-workers other research groups have also studied dry spinning of P(L)LA. Horáček and Kalíšek [1994a] have dry-spun and hot-drawn P(L)LA (M_v = 3.5 x 10^5 g/mol). They dissolved polymer in chloroform. The

highest tensile strength was 0.7 GPa at the draw temperature of 170ºC. They [Horáček & Kalíšek 1994b] have also tried the binary solvent/non-solvent system in dry spinning, but the mechanical strength was not as high as with the solvent system. Precipitant vapor had effect on the degradation rate of dry-spun, hot-drawn filaments [Horáček & Kalíšek 1994c]. Methanol as the precipitant vapor accelerated most the degradation rate of polymer.

Furthermore, Fambri and co-workers [1994] have studied dry spinning and hot drawing of P(L)LA (M_v = 6.2 x 10^5 g/mol). Polymer was dissolved in chloroform, extruded at room temperature, and hot-drawn at temperatures ranging from 150 to 210ºC. The maximum modulus was 10 GPa and tensile strength 1.1 GPa at draw temperature of 200ºC. The degree of crystallinity ranged from 18 to 35 % depending on the draw temperature.

In addition, Tsuji and co-workers [1994] have studied the stereocomplex formation of dry-spun P(D)LA (M_v = 3.0 x 10^5 g/mol) and P(L)LA (M_v = 3.1 x 10^5 g/mol) mixture. They dissolved polymers in chloroform, and the spun fibers were drawn in the temperature range from 120 to 160°C and annealed at the same temperature. The T_m of stereocomplex crystals were up to 230ºC, whereas it was up to 180ºC for single polymers. The maximum tensile strength was 0.9 GPa and modulus 8.7 GPa at the draw ratio of 13 and the drawing temperature of 160ºC.

2.2.3 Wet Spinning

The wet spinning process is similar as the dry spinning process but the polymer solution is pumped through the spinneret into the spin bath (or the coagulation bath) which contains non-solvent of the fiber polymer and possible additives. Wet spinning is the only possible spinning method when the polymer is dissolved in low volatile solvent. The schematic drawing of wet spinning equipment is presented in Figure 5. After coagulation the filaments are removed from the bath and they are washed free from coagulants.

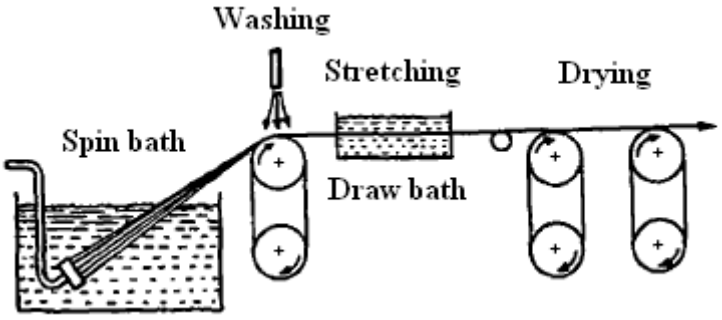

Figure 5 Schematic drawing of laboratory-scale wet-spinning equipment [Frushour & Knorr 2007].

Wet spinning can be divided into the liquid-crystal method, the gel method, and the phase-separation method which are based on different physicochemical principles [Tsurumi 1994]. In the liquid-crystal method, a lyotropic polymer solution is solidified through the formation of a solid crystalline region in the solution. In the gel method, polymer solution is solidified through the formation of intermolecular bonds in the solution. In the phase separation method, two different phases are present in the solution, the polymer-rich phase and the solution-rich phase.

Cupro-cellulose filaments have been produced by wet spinning as early as 1900 [Fourne, p. 498]. Viscose rayon is the other example of the typical wet-spun textile fiber. Many synthetic fibers, which are produced by the dry spinning process, can be produced also by the wet spinning process. The linear speed of commercial wet-spun filament production is very slow compared to the melt spinning production. The spinning capacity can be increased using many spinnerets in the same spin bath. For example, the spinneret for fine viscose fiber contains 30 000 – 50 000 holes and the diameter of each hole is 40 - 50 μm [Wilkes 2001].

The wet spinning method is very practical for solution-polymerized polymers, but it can also be utilized for other polymers which can be prepared to a homogeneous solution.

If polymer is in a solid state, the first step in wet spinning is the polymer dissolving. Polymer dissolves in solvent when dissolution lowers the free energy (ΔG_M). The free energy of mixing must be zero or negative for the solution process to occur spontaneously. The dissolution of polymer into solvent lowers the free energy of the

polymer-solvent system when the enthalpy (ΔH_M) decreases by dissolution or, if it does not, when the product of temperature (T) and the entropy of mixing (ΔS_M) are greater than the enthalpy of mixing. The free energy change for the solution process is given by the Equation 1.

$$\Delta G_M = \Delta H_M - \Delta T S_M \quad (1)$$

where ΔG_M is the free energy of mixing, ΔH_M is the enthalpy of mixing, T is the absolute temperature, and ΔS_M is the entropy change in the mixing process.

Solubility parameters can be used for predicting the solubility of the polymers. The difference in solubility parameters for the solvent-solute combination is important in determining the solubility of the system. Solubility parameters are derived from the energy required to convert a liquid to a gas. The energy of vaporisation is a direct measure of the total energy holding the liquids' molecules together. The total energy consists of several parts, and they arise from dispersion forces, permanent dipole-permanent dipole forces, and hydrogen bonding.

The dissolution of the polymers is due to these three different types of interactions. The most common is the dispersion interaction which arises from atomic forces. The second type is interaction between two permanent dipoles, and the third is hydrogen bonding which are both molecular interactions. It is possible to measure cohesive energies for these three interactions. Further, Hansen solubility parameters (HSP) can be calculated from the energies. [Hansen 2000] Solubility parameters consist of dispersion (δ_d), polar (δ_p), and hydrogen (δ_h) components. The total solubility parameter (δ_{total}) can be conducted from the three components as in Equation 2.

$$\delta_{total}^2 = \delta_d^2 + \delta_p^2 + \delta_h^2 \quad (2)$$

Polymers will dissolve in solvents of which solubility parameters are close to their own. Also the molar volume is used as a fourth parameter to describe the solubility. If two solvents have identical solubility parameters, the solvent with lower molecular volume is the better due to its thermodynamical properties. [Hansen 2000]

The total solubility parameter of polylactide is about 20 $MPa^{½}$ [Auras *et al.* 2004; Blomqvist *et al.* 2002]. It depends on the employed determination method and polymer type as shown in Table 1 [Agrawal *et al*. 2004; Schenderlein *et al.* 2004]. The most considerable difference between the polymers is in the hydrogen parameter (δ_h).

Table 1 Solubility parameters for various lactic acid based polymers [1: Schenderlein *et al.* 2004; 2: Agrawal *et al.* 2004].

Polymer	*Hansen Solubility Parameter ($MPa^{½}$)*				*Determination method*	*Reference*
	δ_d	δ_p	δ_h	δ_{total}		
Poly(D,L-lactide)	15.8	8.7	11.1	21.1	contribution	1
Poly(D,L-lactide)	15.7	3.5	11.1	19.8	turbidity titration	1
Poly(L-lactide)	17.6	5.3	5.8	19.3	intrinsic 3D viscosity	2
Poly(L-lactide)	16.9	9.0	4.1	19.5	classical 3D geometric	2
Poly(L-lactide)	18.5	9.7	6.0	21.7	optimization	2

The solubility of polylactide depends on the molar mass and the degree of crystallinity. Enantiomerically pure P(L)LA is an isotactic polymer and partly crystalline. The increase of D-lactide content in copolymer increases disorder in polymer chains and decreases the degree of crystallinity. Amorphous polymers have less hydrogen bonds between polymer chains. Hence, rasemic and *meso*-lactides are more soluble than enantiomerically pure polylactides [Södergård & Stolt 2002] which can also be conducted from the Hansen Solubility Parameters shown in Table 1.

The good solvents for P(L)LA are chlorinated or fluorinated organic solvents as, for example, chloroform, 1,4-dioxane, 1,3-dioxolane, furan, and pyridine [Södergård & Stolt 2002]. Rasemic and *meso*-lactide are also soluble to other organic solvents, such as propylene carbonate [Schenderlein *et al.* 2004], acetone, ethyl acetate, ethyl lactate, N,N-dimethylformamide, dimethylsulfoxide, methyl ethyl ketone, tetrahydrofurane, and xylene [Södergård & Stolt 2002].

When polymer is in a dissolved form, the spin dope is pumped through the spinneret to the spin bath. The configuration of the spinneret and the spin bath depends on the requirements of polymer, solvent, spin dope concentration, spin bath, and the ease of

handling [Fourne 1999, p. 198]. The spin bath can be flat, deep, or funnel type. Depending on the coagulation and mechanical properties of the solidifying filament, the path of the filament in the spin bath can be upwards, downwards, or the filament direction can be reversed by the guides. In the same spinning line it can be more than one spin bath. The spinning equipment also consists of the drawing and washing baths where solvent is extracted. The drawing of thermoplastic polymers can be separated and done as in the melt spinning process.

The desired spinning pump velocity can be calculated according to Equation 3 [Götze 1967].

$$Q = \frac{Ti \times n \times \upsilon}{\rho \times \frac{\alpha}{100} \times 10000} \tag{3}$$

where Q is the capacity of pump (mL/min), Ti is the desired titer of filaments (dtex), n is the number of the spinneret orifices, v is the velocity of the take-up (m/min), ρ is the density of the spin dope, and α is the concentration of the spin dope (%).

Adding non-solvent to the polymer solution causes the precipitation of the polymer if non-solvent mixes with the good solvent. Suitable non-solvents for polylactide are water, alcohols (methanol, ethanol, and propylene glycol), and unsubstituted hydrocarbons as, for example, hexane and heptane [Södergård & Stolt 2002].

At least three components take part in the solidification of the wet-spun fibers. They are polymer, solvent, precipitating agent (non-solvent), and possible additives. The solidification can be described as the phase diagram of ternary system shown in Figure 6. In the area above the line A, the polymer concentration in the spinning dope decreases and solidification does not occur. To the right of the line B is the area where the spinning solution solidifies through the gel formation or oriented crystals. The liquid-liquid phase separation is not illustrated in Figure 6 but it happens before gel formation and solidification. The phase separation occurs in the area between the lines A and B. This phase separation yields polymer-rich and polymer-lean phases.

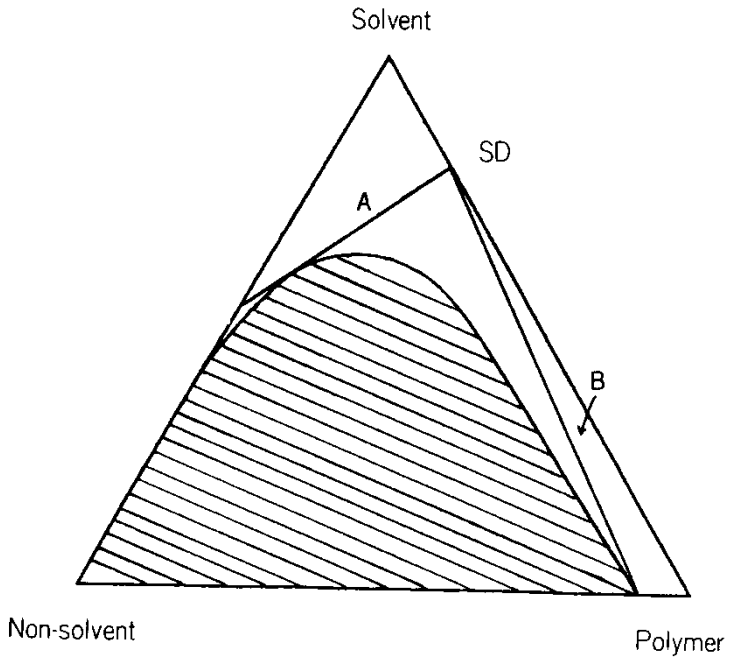

Figure 6 Phase diagram of polymer, solvent, and non-solvent ternary system [Tsurumi 1999].

The normally used coagulation times varies from one second to 15 minutes [Fourne 1999, p. 499]. When the polymer solution comes out from the spinneret the surface layer of the filament forms and then the coagulation continues towards the inside of the filament. The solvent diffuses from the inside of the filament to the surface into the spin bath. During the coagulation, first the gelation should occur, and then the actual phase separation. If the coagulation occurs without the gelation, the intermolecular bonds are not formed and the filaments have low mechanical strength [Frushour & Knorr 2007].

The cross section of the coagulated fiber is affected by the diffusion speed of the coagulation bath. If the amount of solvent diffusing out is greater than the amount of non-solvent diffusing in, the filament core is created an underpressure, and the fiber surface collapses. If the amount of non-solvent diffusing in is greater than the amount of solvent diffusing out, the cross section of fiber remains round. [Frushour & Knorr 2007]

The wet spinning method of polylactide filaments has been introduced as early as 1966 [Kulkarni *et al.* 1966]. The spinning method is not widely used because the wet-spun filaments are not mechanically as strong as melt-spun filaments and the melt spinning process is more economic method than the wet spinning method. However, the novel end-

uses as, for example, in tissue engineering do not need as high filament strength as suture materials or bone fixation devices.

Nelson and co-workers [2003] have studied wet spinning of P(L)LA. They dissolved the polymer in variety of solvent systems, as chloroform, 1,4-dioxane, a mixture of chloroform-toluene, and a mixture of chloroform-hexane. The coagulants, which they used, were isopropyl alcohol, short alkanes (heptane, cyclohexane, hexane, and pentane) and poly(ethylene glycol), and amphiphilic polymers. Their spinning equipment consisted of syringe pump, dispensing needle, glass tube, coagulating bath, and bobbin. The reported ultimate stress values were below 120 MPa. Wet-spun filament bundles have been used to enhance peripheral nerve regeneration across extended nerve lesions [Ngo *et al.* 2003].

Daicel Chemical Industries Ltd. [Ikada & Gen 1991] has patented the filament, which has been made from a blend of P(L)LA and P(D)LA. The spinning methods for producing the filament have been dry spinning, wet spinning, or dry wet spinning. The polymer concentration of a spinning solution has been between 1 - 50 wt%. Examples of organic solvents, which were able to use in wet spinning, were chloroform, methylene chloride, trichloromethane, dioxane, dimethyl sulfoxide, benzene, toluene, xylene, and acetonitrile. The spinning temperature was preferably 20 - 80ºC, and the temperature of a coagulating liquid preferably 0 - 40ºC. As a coagulating liquid it was able to use a single solvent such as methanol, ethanol, acetone, hexane, or water; or a mixture thereof with an organic solvent as used in a spinning solution. The obtained filament was drawn by a dry or wet hot drawing method. The drawing temperature ranged from 100 to 220ºC, preferably 120 - 200ºC. The filament was able to draw by single or multiple stage drawing, however, multiple stage drawing was preferred.

Tsuji and co-workers [1994] have studied wet spinning of P(L)LA (M_v = 3.1 x 10^5 g/mol) and P(D)LA (M_v = 3.0 x 10^5 g/mol) blend to achieve stereocompex type polylactide. They dissolved the polymers in chloroform. The first spin bath contained the mixture of ethanol and chloroform (10/3), and in the second bath the mixing ratio was 10/1. According to the authors, the tensile strength of wet-spun stereocomplex fibers was very low, and the authors were not able to draw the fibers at high temperature.

2.2.4 Dry Wet Spinning

In a combined dry wet spinning process the fibres are pumped through the spinneret first to the air gap, and secondly immersed into the spin bath, as shown in Figure 7. This process is suitable for spinning, for example, lyocell and anisotropic solutions of polyaramides.

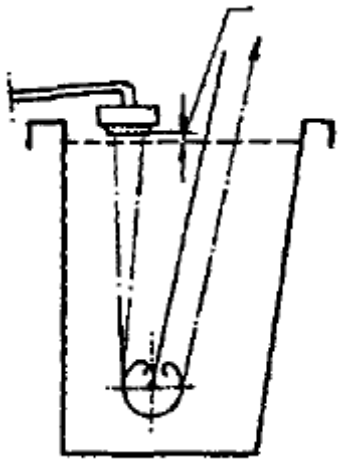

Figure 7 Schematic drawing of dry wet spinning process [Fourne 1999, p. 499].

Gupta and co-workers [2006a; 2006b] have fabricated filaments by the dry wet spinning method. P(L)LA (M_v = 1.53 x 10^5 g/mol) was dissolved in chloroform and coagulated in methanol. The air gap between the spinneret and coagulation bath was adjusted to 25 mm. The filaments were subjected to drawing process at the temperature of 90ºC, and the filaments were heat-setted at 120ºC. The highest modulus was 8.2 GPa and tensile strength was 0.6 GPa. The degree of crystallinity was about 40%.

2.2.5 Wet Spinning of Drug-Loaded Filaments

Both dry spinning and wet spinning processes can be performed at room temperature. It gives two benefits for these spinning processes: polymer is not exposed to a thermal degradation and filaments can be loaded with thermo-sensitive drugs.

The production methods of drug-loaded wet-spun filaments can be divided to one-component and bi-component methods. The bi-component filaments can be fabricated by the double extrusion pump and tube-in-orifice spinneret [Houis *et al.* 2008]. The fabricated bi-component filaments have a core-sheath structure.

The dry wet spinning method has been used to the fabrication of porous P(L)LA filaments for drug delivery systems [Van de Witte *et al.* 1993]. The utilized solvent-nonsolvent system affected on the porosity of filaments. The dense sheath and porous core were formed by the dioxane/water –system, whereas the fully porous structure was formed by the chloroform/toluene-methanol –system. The drug release rate was higher from the porous structure and lower from the dense structure.

Greidanus and co-workers [1990] have patented the similar system as in the previous paragraph has been described. The patent included the biodegradable polymer substrate which was loaded with active substance, like hormone. The porous substance has been fabricated by wet spinning or dry wet spinning. The porosity of filament can be controlled by the solvent/coagulant –system.

Bezemer and co-workes [2004] have patented the process of producing biopolymer filament loaded with a bioactive agent using the wet spinning technique. A water-in-oil emulsion was prepared by mixing the polymer solution with an aqueous solution of the bioactive agent. They added conventional stabilizers for enhancing the stability of the water-in-oil emulsion. Then the water-in-oil emulsion was immersed to the coagulation bath as in the conventional wet spinning method.

Stack and co-workers [1996] have patented the method of making the bioabsorbable stent. The filaments of the stent were able to produce by wet spinning. In this method polymer and drug were not mixed during the extrusion but the filament was covered by drug during the coagulation process. The fibers were run through a post-coagulation bath where the desired drug was able to incorporate into the fibers. The pores, which were formed during the coagulation, were able to partially collapse by stretching, heating, or solvent exposure thereby trapping the drug throughout the filament. If a heat sensitive drug was incorporated, then subsequent processing steps must avoid high temperature, for example, the heat setting step was able to replace by chemical setting.

Gao and co-workers [2007] have used similar wet spinning configuration as Nelson and co-workers [2003]. The drug (5-fluorouracil) was micronized by fluid jet mill and the particle size was in the range of 0.5 - 5 μm. The drug was dispersed in chloroform with a dispersing agent (Span 80) by a bath sonicator. They dissolved P(L)LA in suspension and coagulated the filaments in isopropyl alcohol or a mixture of isopropyl alcohol and methanol.

Crow and Nelson [2006] have fabricated core-sheath P(L)LA filament by a bi-component wet-spinning technique. The outer core consisted of bovine serum albumin (BSA) and albumin gel. The BSA has been used as a model to the growth factors. The inner core consisted of polymer, and it was dissolved in chloroform. The coagulant was pentane. The same technique has been described in the study of Crow and co-workers [2005]. They [Nelson & Crow 2006] have also patented their method to fabricate a gel or hydrogel loaded biodegradable filament.

Polacco and co-workers [2002] have produced hollow wet-spun filaments containing drug-loaded nanoparticles by a bi-component spinning method. The filament polymer was poly(DL-lactide)-*co*-poly(ε-caprolactone), which was dissolved in acetone. The cogulation bath consisted of deionized water. The outer sheath was formed from polymer, and the core has been consisted of the drug-loaded particle for producing bi-component filaments. The particles were prepared oil-in-water and water-in-oil emulsification process from poly-(DL-lactide-*co*-glycolide) and gelatin. The oil phase and the aqueous phase were mixed with a high-speed homogenizer.

The same research group [Lazzeri *et al.* 2005] has produced also drug-loaded hollow P(L)LA microfilaments by dry wet spinning method. The polymer solvent was chloroform and the filaments were coagulated by a phase inversion mechanism due to evaporation of chloroform and precipitation of water, which was inside the filament.

Wet spinning has also used for producing, for example, drug-loaded chitosan filaments [Denkbas *et al.* 2000], alginate filaments [Miraftab *et al.* 2003], sheat-core polyurethane filaments [Hussain *et al.* 1989], and DNA-films [Fritzsche *et al.* 1984].

2.2.6 Electrospinning

Nano-scale fibres can be produced by electrospinning, which is a drawing process based on electrostatic interactions. A solid filament is formed from a highly viscous polymer solution by the electrified jet. [Li & Xia 2004] There are two main methods for producing highly viscous polymer ready for electrospinning: dissolving and melting. The dissolving method in electrospinning is the traditional method, and it enables filament loading with thermo-sensitive drugs, whereas the melt electrospinning technique is more suitable for continuous spinning lines. The basic principle of electrospinning is illustrated in Figure 8.

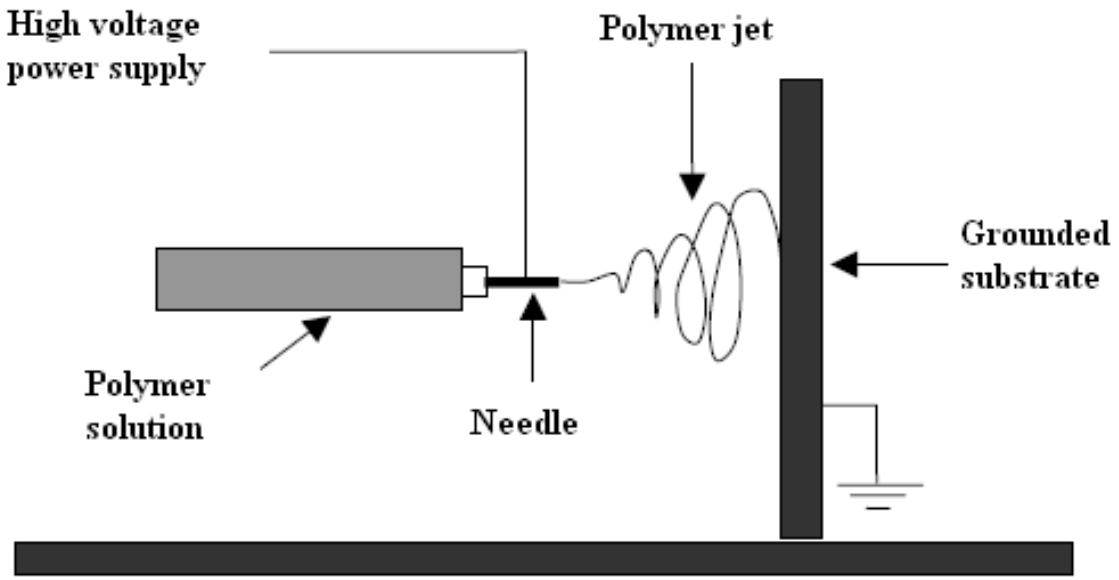

Figure 8 Schematic drawing of electrospinning equipment [Freenam *et al.* 2008].

Electrospinning of P(L)LA has been widely studied [Yang *et al.* 2004, Yang *et al.* 2005, You *et al.* 2005, He *et al.* 2006, Li *et al.* 2006, Ogata *et al.* 2006, Zhou *et al.* 2006, Zhmayev *et al.* 2008, Wang *et al.* 2008]. Tsuji *et al.* [2006] have studied the electrospinning of stereocomplex type polylactide. The stereocomplexation has been increased the T_m of electro-spun fibers as it has been mentioned with normal-scale fibers. The studies concerning the electrospinning of polylactide have mainly focused on manufacturing of scaffolds in tissue engineering, because nano-scale filaments promote the cell growth [Ndreu *et al.* 2008].

3 MATERIALS AND METHODS

In this chapter all materials, which were used in the research reported in this thesis, are described. Furthermore, the solubility and phase separation studies prior to the spinning studies are explained. The experimental work considering fiber forming and characterization is described in detail.

3.1 MATERIALS

The polymers were medical grade polylactide stereo copolymers. One P(L/D)LA copolymer, L to D ratio 50/50 was purchased from Boehringer Ingelheim Pharma GmbH & Co, Ingelheim am Rhein, Germany. Two P(L/D)LA copolymers, L to D ratio 96/4, and one P(L/DL)LA copolymer, L to DL ratio 70/30, were purchased from Purac Biochem bv, Gorinchem, The Netherlands. The polymers, their molar masses, and inherent viscosities (IV) are shown in Table 2. The molar masses were determined by gel permeation chromatography [Ellä *et al.* 2005]. The IV values were given by the polymer supplier.

Table 2 Polymers, their molar masses and inherent viscosities.

Paper	*Polymer*	*Molar mass (kg mol^{-1})*			*IV*
		M_v	M_n	M_w	*(dL/g)*
I, II, III, IV	P(L/D)LA, L/D ratio 96/4	94	55	100	2.2
I	P(L/D)LA, L/D ratio 96/4	250	150	270	4.8
I, II, III, IV	P(L/DL)LA, L/DL ratio 70/30	170	100	180	3.1
I	P(L/D)LA, L/D ratio 50/50	-	130	240	1.6

Eight analytical grade polymer solvents and four non-solvents were used in the experiments. The solvents were acetone, dichloromethane, 1,4-dioxane, formic acid (98 %), methyl acetate, propylene carbonate, pyridine, and tetrahydrofurane. The analytical grade non-solvents were methanol, ethanol, isopropyl alcohol, and *n*-hexane. Bovine serum albumin, minimum 96 % electrophoresis, was purchased from Sigma-Aldrich Co. (Saint Louis, USA).

3.2 SOLUBILITY AND PHASE SEPARATION STUDIES

3.2.1 Solubility Experiments

The solubility was tested in test tubes and determined by visual observation [Schenderlein *et al.* 2004]. Each polymer sample was weighed (0.2 g) in the test tube and 2.0 ml of solvent was measured to the test tube. They were closed instantly with polytetrafluorethylene coated stoppers to prevent evaporation of the solvent. The test tubes were shaken after 1 hour. The solubility was defined visually after 24 hours. The interaction between the polymer and the solvent was classified into six groups. The scale was from 1 to 6: 1-clear solution, 2-gel-like, thread-shaped structures, 3-solid, gelatinous, 4-very swollen, 5-slightly swollen, 6-insoluble, as shown in Figure 9.

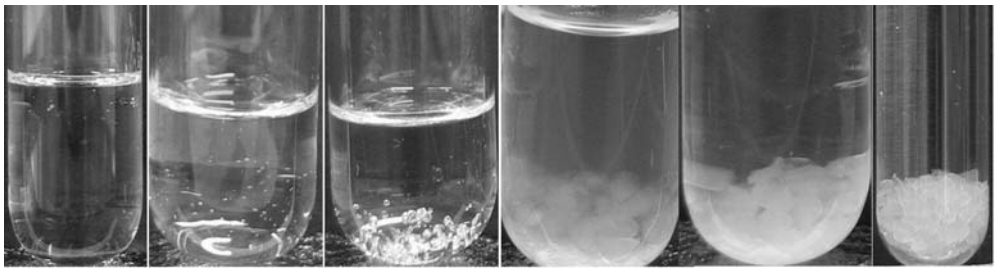

1 2 3 4 5 6

Figure 9 Examples from the scale: 1-clear solution, 2-gel-like, 3-gelatinous, 4-very swollen, 5-slightly swollen, and 6-insoluble.

3.2.2 Cloud Point Titration

The cloud points of the solvent-polymer-non-solvent mixtures were evaluated using titration [Hausberger & DeLuca 1995; Murakami *et al.* 2000; Schenderlein *et al.* 2004]. Three different amounts (0.3, 0.8 and 1.3 g) of polymer materials were used. The polymer was dissolved in 10.0 ml of dichloromethane in a conical flask with a glass stopper at room temperature. The titration was stopped at the first visually observed sign of precipitation.

The volumes of non-solvents in the cloud point were converted to mass units. The non-solvent percentage in the polymer solution at the cloud point, CL_{ns}, was determined as an index [Hausberger & DeLuca 1995; Murakami *et al.* 2000].

3.3 FILAMENT MANUFACTURING

3.3.1 Spin Dope Preparation

The polymer granules were dissolved in dichloromethane in a conical flask covered by a glass stopper at room temperature by a magnetic stirrer until the polymer solution was clear. Air bubbles were removed from the polymer solution by standing it. The spin dope concentrations were calculated from the volume of the solvent. Viscosities of polymer solutions were measured by Brookfield DV-II+ viscometer. The spin dope concentrations and viscosities are given in Table 3.

Table 3 Spin dopes and molar masses of wet-spun filaments.

Polymer	*Material type*	*Paper*	*Molar mass (M_v / kg mol $^{-1}$)*	*Spin dope concentration (%)*	*Spin dope viscosity (cP)*
P(L/D)LA	Filament	II, III	98	15	1720
96/4	Protein-loaded	IV	-	10	-
P(L/DL)LA	Filament	II, III	170	10	1660
70/30	Protein-loaded	IV	-	8	-

BSA was dissolved in distilled water. The amount of BSA was 2 % from the weight of polymer and the volume of water was 6 % from the volume of dichloromethane. The polymer solution and the protein solution were probe sonicated (Dr. Hielscher UP200S, Teltow, Germany) to form emulsion. A cooled (5°C) metal container was used to limit the heating of the mixture. The probe sonicator was used to mix the polymer solution and water solution because it generated small protein-water dispersion into the polymer solution.

3.3.2 Wet Spinning

The polymer solution was decanted from the conical flask to the spinning tank. The polymer solution was pumped (Zenith gear pump made by Allweiler AG, Radofzell, Germany) through the spinneret (20 holes, hole diameter 0.1 mm; Enka Technica GmbH, Heinsberg, Germany) into the coagulation bath. The used precipitants were analytical grade methanol or ethanol. The filaments were reeled to the bobbin (diameter 87 mm) coated by a plastic film. The schematic drawing of the wet spinning equipment is presented in Figure 10. The utilized spin draw ratios (SDR) were from 1.4 (low) to 9.8 (high) and they were calculated from the ratio of the final velocity (reeling velocity) and the initial velocity (spinneret velocity). The spinneret velocities were in the range of 7 - 30 m/min and the reeling velocities were 9 – 70 m/min respectively, as presented in Table 4.

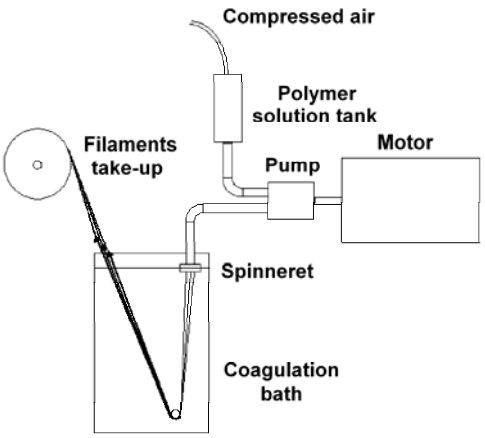

Figure 10 Schematic drawing of wet spinning equipment.

The protein-loaded filaments were manufactured by the similar spinning equipment as the unloaded filaments. The spinneret had 10 holes, and the hole diameter was 0.15 mm (Enka Technica GmbH, Heinsberg, Germany). The ethanol containing coagulation bath was used for the protein-loaded filaments. The utilized spinneret velocity was 6.3 m/min and the reeling velocity was 9 m/min, as presented in Table 4.

Table 4 Spinning parameters of wet-spun filaments.

Filament	*Spin draw ratio*	*Pump velocity (m/min)*	*Reeling velocity (m/min)*	*Coagulation time (s)*	*Spinneret type (holes x hole diameter in mm)*
Spin-drawn filaments (paper II)	1.4	7.1	10	5.6	20 x 0.1
	1.4	21.4	30	1.9	
	4.2	7.1	30	2.6	
	7.0	7.1	50	1.7	
	9.8	7.1	70	1.2	
As-spun filament (paper III)	1.4	7.1	10	5.6	20 x 0.1
Protein-loaded filament (paper IV)	1.4	6.3	9	7.1	10 x 0.15

The separate hot drawing was done using the heated oven with air-gap. The utilized hot draw ratios were 2.5, 3.0, and 4.5 to P(L/D)LA 96/4 filaments and 2.0 and 3.0 to P(L/DL)LA 70/30 filaments.

The filaments were evacuated in a vacuum oven at 37 - 40ºC overnight to eliminate the chemical residues [Chen *et al.* 2006]. The filaments were stored in a desiccator until their testing to avoid the moisture intake.

3.4 FILAMENT CHARACTERIZATION

3.4.1 Filament Morphology

Scanning electron microscope (SEM) (Jeol JSM-T100, Jeol Ltd., Tokyo, Japan) was used to characterize filament surface and cross-sectional specimens. The cross-sectioning of the specimens was performed by cutting filaments in liquid nitrogen. The specimens were coated with a thin gold layer.

3.4.2 Thermal Properties

A heat-flux type differential scanning calorimeter (DSC) 821^{TM} from Mettler Toledo Inc. (Columbus, Ohio, USA) was used for measurements of thermal behaviour of the

copolymer granules and the filaments. In DSC the difference in the amount of heat required to increase the sample temperature and reference are measured as a function of temperature. The glass transition temperatures (T_g), the peak melting temperatures (T_m), the crystallization enthalpies (H_c), and the melting enthalpies (H_m) were measured at a heating rate of 10 K min^{-1}. Two to four parallel sets of samples (about 5 mg) were heated from -10 to 250°C in standard 40 µl aluminium sample crucibles. Data were taken from the first heating scans. The degree of crystallinity was calculated as in Equation 4.

$$X_c = (\Delta H_c + \Delta H_m) / 0.937 \quad (4)$$

where X_c is the degree of crystallinity, ΔH_c is the crystallization enthalpy and ΔH_m is the melting enthalpy. The value of ΔH_m = 93.7 J/g was used for the totally crystallinized polylactide crystal [Fischer *et al.* 1973].

If the post-crystallization, that is cold-crystallization, was observed in the DSC-curve, the initial degree of crystallinity was calculated as in Equation 5.

$$X = X_c - X_{cc} \quad (5)$$

where X is the initial degree of crystallinity and X_{cc} is the degree of post-crystallization.

3.4.3 Fiber Fineness

Fiber fineness was determined by measuring the fiber diameter and the linear density, which is the weight per unit length. The fiber diameter is a useful way to define the fineness for fibers, which are circular in cross section and which do not vary in thickness along their length. The linear density is a useful way to describe fineness of fibers, which are not circular in cross section.

The fiber diameter was determined by a projection microscope (Projectina, Projectina AG, Heerbrugg, Swizerland) from 50 individual filaments. The fiber diameter was expressed by microns (µm).

The linear density was determined by Vibroskop (Lenzing AG, Lenzing, Austria) from 50 individual filaments, and it was expressed in terms of dtex (the weight in grams of 10 000 metres). In the vibroscope method the fiber under specified tension was subjected to vibration at resonance frequency. The linear density of the filament was read directly on the scale of the vibroscope apparatus.

Vibroscope method is based on the fact that for a perfectly flexible string of mass per unit length m and length l, under tension T, the natural frequency of transverse vibration, f, is given by Equation 6 and 7.

$$f = \frac{1}{2l}\left(\frac{T}{m}\right)^{1/2}(1+a), \tag{6}$$

whence:

$$m = T\left(\frac{1}{2lf}\right)^{2}(1+a)^{2} \tag{7}$$

where a is a correction factor involving the elastic modulus of the material. If a is small, then m can be found for a specimen of fixed length, l, by varying tension, T, until a given natural frequency, f, is obtained. [Morton & Hearle 1997, p. 143]

3.4.4 Mechanical Properties

The engineering stress-strain behaviour was measured by the Vibrodyn tensile testing machine (Lenzing AG, Lenzing, Austria). The Vibrodyn machine gives the engineering stress values in cN/dtex. They were converted to MPa by dividing the force by the original cross-sectional area of fiber as in Equation 8.

$$\sigma = \frac{F}{A_0} \tag{8}$$

in which σ is engineering stress, F is the load applied to the specimen, and A_0 is the original cross-sectional area before any load is applied.

The engineering strain, ε, is expressed as in Equation 9.

$$\varepsilon = \frac{\Delta l}{l_0} \times 100 \tag{9}$$

in which l_0 is the original length before any load is applied, and Δl the change in length.

The Vibrodyn machine gave also the breaking force, Young's modulus, and elongation at break values. Breaking force is defined as a maximum force applied to the test specimen carried to a rupture during the tensile test, Young's modulus as the ratio of stress over strain in the range of stress in which Hooke's law holds, and the elongation at break as elongation of the test specimen produced the breaking force.

According to the testing procedure, 50 individual fibers were extended at a constant rate until a rupture occurred. The elongation of the fiber and the force required were measured. The gauge length (initial length) was normally 20 mm. If the elongation at break was over 200%, the gauge length was adjusted to 10 mm, so that the fibre had enough space to the elongation. The speed of the moving clamps was 20 mm/min. The maximum force of the load cell was 100 cN. The recommended pretension of the Vibrodyn manufacturer was used (about 1.0 ± 0.1 cN/tex).

3.4.5 *In vitro* studies

For *in vitro* degradation studies the filament bundles were placed in test tubes and the tubes were filled with 10 ml of soaking solution (phosphate buffer solution) [Shah *et al.* 1992]. The filled test tubes were kept at constant temperature (37 ± 1ºC). The soaking solution was changed during the testing time to maintain a pH of 7.4 ± 0.1. The tensile properties were tested from 20 individual wet filaments at each data point. The data points of each filament types are presented in Table 5.

Table 5 *In vitro* data points for each filament types.

Paper	*Filament type*	*Study time period (weeks)*
II	Spin-drawn	0, 2, 4, 6, 8, 12, 16, 20, 24, and 52
III	Hot-drawn	0, 2, 4, 6, 8, 12, 16, 20, 24, and 52
IV	Protein-loaded	1, 2, 3, 5, 9, 13, 17, 21, and 24

For *in vitro* protein release study the three parallel filament bundles (500 mg) were placed in test tubes, and the tubes were filled (5 ml) with soaking solution (phosphate buffer solution) [Shah *et al.* 1992]. The testing conditions were similar to the *in vitro* degradation studies. Samples of 5 ml solution were collected periodically (Table 5) and their BSA contents were determined via a standard curve by measuring absorbance at 279.0 nm, with the use of a Unicam UV 540 spectrometer (Thermo Spectronic, Cambridge, UK). Finally, a fresh soaking solution of 5 ml was transferred to the test tubes.

4 RESULTS AND DISCUSSION

This chapter summarizes the most significant findings made in Papers I – IV. Firstly the solubility and phase separation studies are presented, and then the characterization results of wet-spun, hot-drawn, and protein-loaded fibers are reported and discussed.

4.1 SOLUBILITY AND PHASE SEPARATION

The solubility of copolymers and their phase separation ability were tested prior to filament spinning, and it is studied in Paper I. The tested solvents and non-solvents were chosen based on the literature and their possibility to utilize in wet spinning. The results of solubility experiments are shown in Table 6. Dichloromethane dissolved all the tested polymers. Respectively, P(L/D)LA 50/50 was soluble in every tested solvent. As expected, none of non-solvents dissolved any polymer.

Table 6 Solubility of tested polymers in various solvents and non-solvents (scale: 1-clear solution, 2-gel-like, 3-gelatinous, 4-very swollen, 5-slightly swollen, and 6-insoluble).

	Polymer			
	P(L/D)LA 96/4 IV=2.2 dL/g	*P(L/D)LA 96/4 IV=4.8 dL/g*	*P(L/DL)LA 70/30*	*P(L/D)LA 50/50*
Solvent				
1,4-Dioxane	3	4	3	1
Propylene carbonate	6	5	4	1
Tetrahydrofurane	4	5	3	1
Pyridine	3	5	3	1
Methyl acetate	5	5	3	1
Acetone	5	5	3	1
Dichloromethane	1	1	1	1
Formic acid (98 %)	5	5	2	1
Non-solvent				
n-Hexane	6	6	6	6
Isopropyl alcohol	6	6	6	6
Ethanol	6	6	6	5
Methanol	6	6	6	5

The solubility of analyzed copolymers was clearly dependent on the L to D ratio of the polymer. From the tested polymers P(L/D)LA 96/4 contained the lowest amount of D-lactide, and it was only soluble in dichloromethane. On the other hand, P(L/D)LA 50/50 contained the highest amount of D-lactide, and it was soluble in all eight solvents. The solubility of P(L/DL)LA 70/30 copolymer was between these two above mentioned copolymers. The high number of D-segment in the polymer structure increases the amorphous region of copolymer, and normally the solvent penetrate first to the amorphous region. The given solubility results are in accordance with previous findings [Schenderlein *et al.* 2004; Södergård & Stolt 2002].

The analyzed P(L/D)LA 96/4 copolymer had two different molar masses (M_v), and thus two different inherent viscosities (2.2 and 4.8 dL/g) and. These samples had only small differences in solubility. The P(L/D)LA 96/4 copolymer (IV 2.2 dl/g) was slightly more soluble than the copolymer with higher inherent viscosity (IV 4.8 dl/g). The lower molar mass of P(L/D)LA 96/4 (IV 2.2 dl/g) promotes the solubility and solvent molecules were more easily able to penetrate inside the copolymer.

The solubility results can be conducted from Hansen solubility parameters although any computational program was not used for the prediction. The Hansen solubility parameters and the molar volumes of the tested solvents and non-solvents are given in Table 7. The solubility parameters of tested copolymers were not known, but presumably they are between the values of polymers, which are given in Table 1. Dichloromethane (Table 7) and polymers (Table 1 on page 17) have similar solubility parameters. Also dichloromethane has low molar volume which promotes solubility. On the other hand, the parameters of propylene carbonate are dissimilar and it has high molar volume. The analyzed polymers were least soluble in propylene carbonate from the tested solvents.

Table 7 Hansen solubility parameters and molar volumes for tested solvents and non-solvents (Hansen 2000).

	Hansen Solubility Parameter ($MPa^{1/2}$)				*Molar volume ($cm^3\ mol^{-1}$)*
	δ_d	δ_p	δ_h	δ	
Solvent					
1,4-Dioxane	19.0	1.8	7.4	20.5	85.7
Propylene carbonate	20.0	18.0	4.1	27.3	85.0
Tetrahydrofurane	16.8	5.7	8.0	19.4	81.7
Pyridine	19.0	8.8	5.9	21.8	80.9
Methyl acetate	15.5	7.2	7.6	18.7	79.7
Acetone	15.5	10.4	7.0	20.0	74.0
Dichloromethane	18.2	6.3	6.1	20.3	65.3
Formic acid (98 %)	14.3	11.9	16.6	24.9	37.8
Non-solvent					
n-Hexane	14.9	0.0	0.0	14.9	131.6
Isopropyl alcohol	15.8	6.1	16.4	23.6	76.8
Ethanol	15.8	8.8	19.4	26.5	58.5
Methanol	15.1	12.3	22.3	29.6	40.7

Because all the copolymers were soluble in dichloromethane, it was used for the cloud point titration experiments. All the analyzed non-solvents were miscible with dichloromethane. Dichloromethane and *n*-hexane are hydrophobic, whereas the analyzed alcohols are water soluble.

The dependencies of CL_{ns} on the polymer concentration are represented in Figure 11 and Figure 12. When the polymer concentration increased, the non-solvent concentration decreased in the precipitation point. *N*-hexane was the most efficient non-solvent for both tested polymers. The cloud points of ethanol and methanol were close to each other. Isopropyl alcohol was the least efficient coagulant from the tested non-solvents.

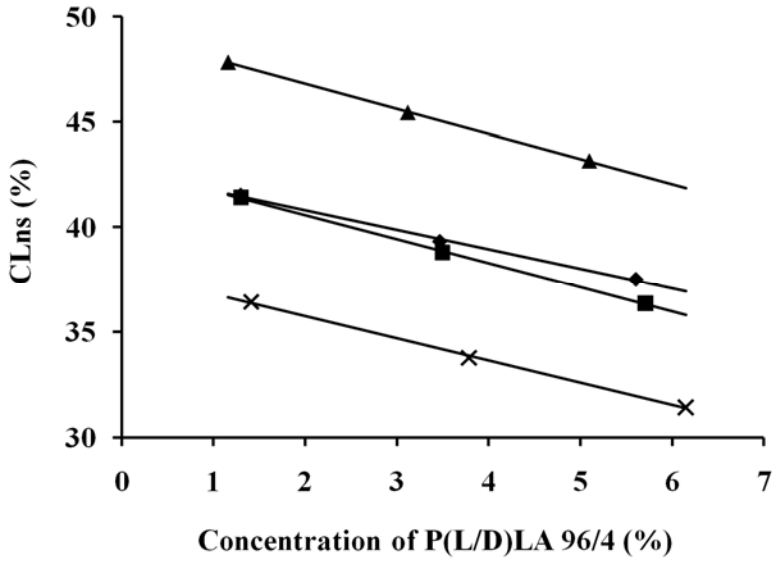

Figure 11 Dependence of CL_{ns} on the concentration of P(L/D)LA 96/4 (IV 2.2 dl/g) in various non-solvents: (♦) methanol, (■) ethanol, (▲) isopropyl alcohol, and (x) *n*-hexane.

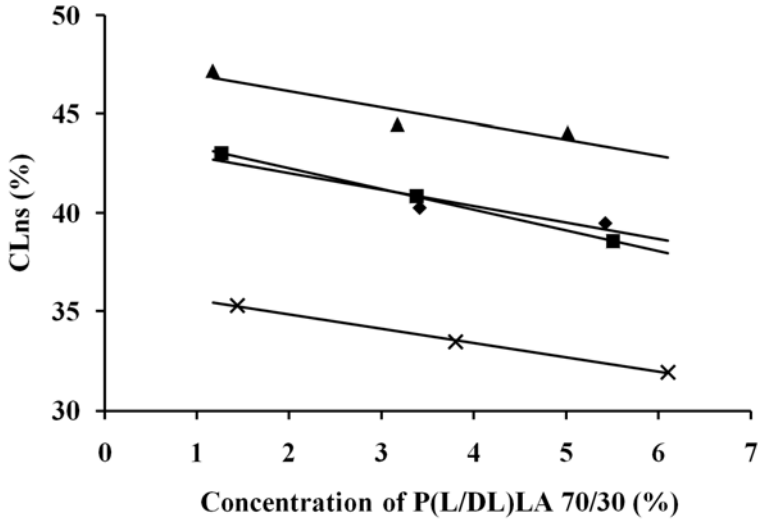

Figure 12 Dependence of CL_{ns} on the concentration of P(L/DL)LA 70/30 in various non-solvent: (♦) methanol, (■) ethanol, (▲) isopropyl alcohol, and (x) *n*-hexane.

The size and shape of non-solvent molecules were important factors in the phase separation. Smaller and more linear molecule, like *n*-hexane, diffused more rapidly than larger and bulkier molecules, like alcohols. Alcohols formed bigger aggregates, and their diffusion was more difficult than the diffusion of linear molecules.

The cloud point titration results showed that the phase separation ability can also be deduced from the solubility parameters shown in Table 1 and Table 7. *N*-hexane had the highest molar volume from the analyzed non-solvents and its solubility parameters differed from the parameters of polylactides given in other researchers presented in Table 1 [Agrawal *et al.* 2004; Schenderlein *et al.* 2004]. Although the differences in CL_{ns} of P(L/D)LA 96/4 and that of P(L/DL)LA 70/30 were not big, the phase separation of P(L/D)LA 96/4 would occur most rapidly because the analyzed non-solvents were further away from the solubility gap of polymer.

The cloud point titration results can be utilized in wet spinning. The fiber formation occurs more instantly from higher polymer concentrations. However, the selection of the polymer concentration is restricted, because the practical polymer solution viscosity gives the upper and lower limits for utilized polymer concentration. The targeted fiber diameter also defines the limits. In a spin bath, solvent and non-solvent are mixed together, and the solidification of polymer will occur quite instantly, but gradually. In the beginning, when the amount of non-solvent is low in the polymer-rich phase, polymer is in the liquid phase. The increased amount of non-solvent solidifies the polymer. The fibre formation of the tested copolymers would occur most rapidly in the *n*-hexane spin bath. The use of the *n*-hexane spin bath is not practical in the laboratory scale because of its high volatility and flammability. Because of this methanol and ethanol were chosen for the spin bath non-solvents.

4.2 WET SPINNING OF POLYLACTIDE STEREOCOPOLYMERS

4.2.1 Wet Spinning

Wet spinning of polylactide stereo copolymer multifilaments is described in Paper II. Spinning was possible to perform using the reeling velocity as high as 70 m/min without any filament breakages.

The molar masses of filaments were determined after spinning. The viscosity-average molar mass of P(L/DL)LA 70/30 remained same before and after wet spinning as shown

in Table 2 on page 25 and Table 3 on page 27. The molar mass of P(L/D)LA 96/4 slightly increased after wet spinning. Probably the dissolution process had an effect on the polymer chains because the polydispersity (PD) value slightly decreased ($PD_{polymer}$ = 1.8; $PD_{filament}$ = 1.7) after spinning. Because the wet-spun filaments were processed at room temperature the polymer did not degrade as in the melt spinning process. Since melt-spun filaments are processed at elevated temperature, the molar mass can decrease significantly due to the thermo-oxidative degradation caused by direct heating, conversion of mechanical energy related to screw speed and torque, and the residence time [Wang, Y. *et al.* 2008]. In Table 8 is presented the molar mass decreases during spinning observed in the other studies.

Table 8 Molar mass decreases during spinning.

Spinning method	*Polymer*	*M_v (g mol^{-1})*	*Decrease of M_v (%)*	*Reference*
Melt spinning	P(D)LA	2.8 x 10^5	40	Weiler & Gogolewski 1996
	P(L)LA	42 x 10^5	50	Ferguson *et al.* 1996
	P(L)LA	3.3 x 10^5	70	Fambri *et al.* 1997
	P(L/D)LA 96/4	1.0 x 10^5 *	0	Paakinaho *et al.* 2009
	P(L/D)LA 96/4	2.7 x 10^5 *	50	Paakinaho *et al.* 2009
	P(L/D)LA 96/4	3.4 x 10^5 *	63	Paakinaho *et al.* 2009
	P(L/DL)LA 80/20	2.1 x 10^5	60	Ferguson *et al.*1996
	P(L/D)LA 70/30	1.6 x 10^5	50	Ferguson *et al.*1996
Dry spinning	P(L)LA	9.1 x 10^5	25	Postema *et al.* 1990
	P(L)LA	6.6 x 10^5	6	Fambri *et al.* 1994
Dry wet spinning	P(L)LA	1.5 x 10^5	5	Gupta *et al.* 2006a

*) Molar mass is given in M_w.

The reported molar mass decreases have been even 70 % in melt spinning. On the other hand, Paakinaho and co-workers [2009] have reported no decrease in M_w during melt spinning. They have used low-molar-mass polylactide with low melt viscosity. Yuan and co-workers [2001] also noticed the lowest molar mass decrease with polymers having originally lowest molar mass. During dry spinning and dry wet spinning the decreases of molar mass have been lower. The length of the dissolution time has had an effect on the reduction of molar mass. The time has been one week for the dry-spun filaments [Postema *et al.* 1990; Fambri *et al.* 1994] and 24 hours for the dry-jet-wet-spun filaments

[Gupta *et al.* 2006a]. Respectively, the dissolution times were only 1-2 hours in this study.

4.2.2 Hot Drawing

The hot drawing process of the polylactide stereo copolymer multifilaments is described in Paper III. Both copolymers were possible to draw at the temperature of 65°C which is around the T_g of tested polymers (Table 9 on page 43). At this temperature the maximum draw ratio was 4.5 to the P(L/D)LA 96/4 filaments and 3 to the P(L/DL)LA 70/30 filaments. Higher draw temperatures (> 70°C) were also tried, but the filaments shrank and broke [P(L/DL)LA 70/30] or they melted together in the multifilament yarn [P(L/D)LA 96/4].

In the earlier studies much higher draw temperatures has been used to dry-spun P(L)LA filament [Leenslag & Pennings 1987; Postema & Pennings 1989; Eling *et al.* 1987; Fambri *et al.* 1994]. In their studies the optimum hot draw temperature was as high as 200°C, which is near the T_m of P(L)LA. However, their use of thick monofilament enabled the high draw temperature, whereas thin multifilament yarn was used in this study.

4.2.3 Protein Loading

Wet spinning of protein-loaded polylactide stereo copolymer multifilaments is described in Paper IV. The preparation of polymer-protein emulsion increased the viscosity of spin dope, and thus the lower polymer concentration was utilized. The spin dope concentration was 10 % for P(L/D)LA 96/4 and 8 % for P(L/DL)LA 70/30, whereas they were 15 % and 10 % for the unloaded filaments. The fabrication of protein-loaded wet-spun filaments was more difficult than the spinning of unloaded filaments. The polymer emulsion contained very small air bubbles which caused difficulties in filament spinning. For example, the maximum reeling velocity was as low as 9 m/min for protein-loaded filaments, whereas it was as high as 70 m/min for unloaded filaments. Also larger hole diameter, 0.15 mm, was used for protein-loaded filaments.

4.3 PROPERTIES OF WET-SPUN FILAMENTS

4.3.1 Filament Morphology

SEM-images of the P(L/D)LA 96/4 filaments are presented in Figure 13 and those of the P(L/DL)LA 70/30 filaments in Figure 14. The skin-core structure can be observed in all filaments. The outer surface is solid and smooth, whereas the inner core is porous. In the previous studies [Gupta *et al.* 2006a; Gao *et al.* 2007] the wet-spun filaments have been shown a porous structure. The small pores were formed during the coagulation process. The surface of filament was solidified immediately and thus the skin was formed first. Solvent and non-solvent were trapped inside the filament. The porous structure was formed when solvent and non-solvent were evaporated from the filament after the solidification. The phase separation rate of P(L/D)LA 96/4 was slightly faster than that of P(L/DL)LA 70/30 according to the phase separation studies. If the solidification process is fast, the high number of pores is formed. Respectively, the slow solidification rate decreases the formation of pores. [Frushour & Knorr 2007] Although the porosity of filaments was not measured, the P(L/DL)LA 70/30 filaments could be less porous based on the slower solidification rate.

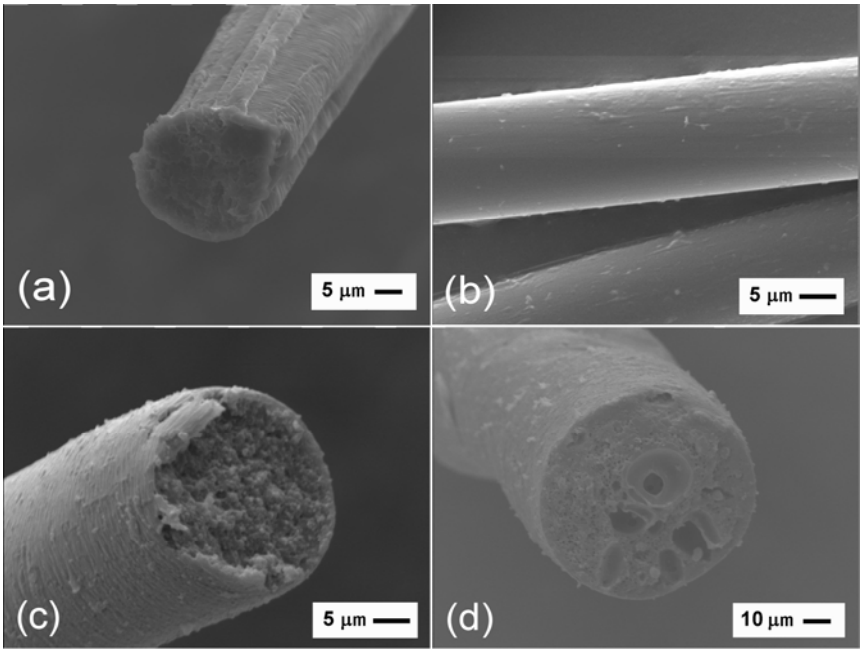

Figure 13 SEM-images of P(D/L)LA 96/4 filaments: (a) spin draw ratio 1.4; (b) spin draw ratio 7.0; (c) hot draw ratio 4.5; and (d) protein-loaded; coagulant: ethanol.

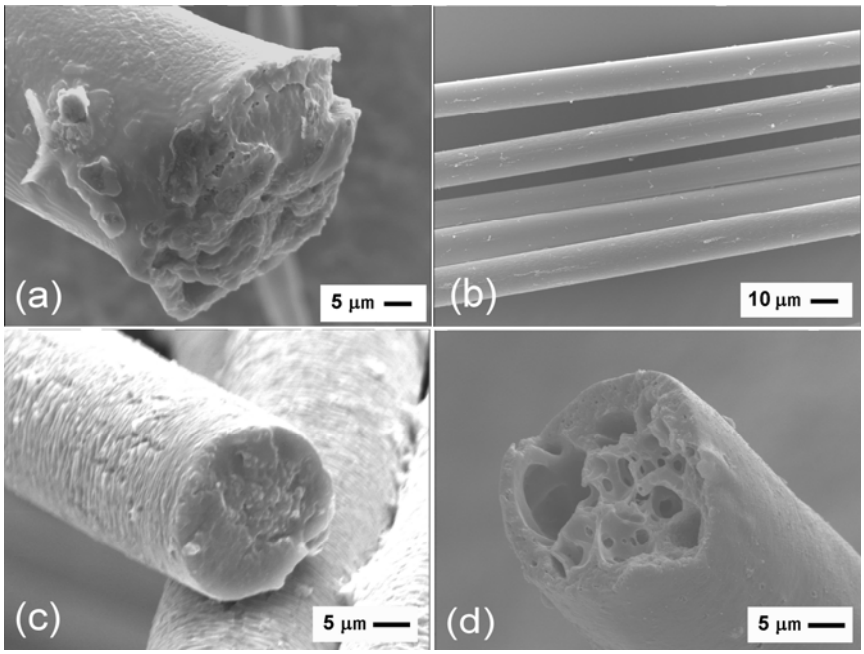

Figure 14 SEM-images of P(D/L)LA 70/30 filaments: (a) spin draw ratio 1.4; (b) spin draw ratio 7.0; (c) hot draw ratio 3.0; and (d) protein-loaded; coagulant: ethanol.

The P(L/D)LA 96/4 filaments with the spin draw ratio 1.4 had distinct collapsed, serrated cross-section (Figure 13a). It was formed when the solidifying outer skin was rigid and more solvent exited the filament than non-solvent entered. The surface of the P(L/DL)LA 70/30 filaments were partly serrated, partly smooth. Because the coagulation rate of the P(L/DL)LA 70/30 filament was slightly slower, the solidifying outer skin was softer and more deformable, and the cross-section of filaments became more circular, as shown in Figure 14a .

The surfaces of the filaments with the spin draw ratio of 7.0 were smooth. The filament drawing orientated the molecular structure and this can be seen in the smooth surface (Figure 13b and Figure 14b). The hot-drawn filaments had smaller diameter, but the appearance was similar as the as-spun filaments (Figure 13c and Figure 14c).

The sonication of the protein-polymer solution formed air bubbles to the spin dope, and thus it can be seen, in addition of small pores, also large pores in the cross-sections of the filaments. The P(L/DL)LA 70/30 filaments (Figure 14d) contained a high number of the

large pores, whereas the P(L/D)LA 96/4 (Figure 13d) filaments had lower number of the large pores.

4.3.2 Crystallinity and Thermal Behaviour

The effect of spin drawing and hot drawing on the degree of crystallinity and the thermal behaviour are studied in Papers II and III. The thermal behaviours and the degrees of crystallinities were measured because they have an influence among the others on the degradation properties. The measured T_g and T_m values, and calculated degrees of crystallinities are presented in Table 9.

Table 9 Glass transition temperatures (T_g), melting temperatures (T_m), and the degrees of crystallinities (X) of granulates and filaments. S = short coagulation time, L = long coagulation time.

Material	*Spin draw ratio*	*Hot draw ratio*	*T_g (°C)*	*T_m (°C)*	*X (%)*
P(L/D)LA 96/4					
Granulate	-	-	65 – 68	157	40
Filament, Met-OH, S	1.4	-	66	157	16
Filament, Met-OH	7.0	-	70	156	14
Filament, Met-OH	9.8	-	70	157	12
Filament, Et-OH, S	1.4	-	66	157	16
Filament, Et-OH, L	1.4	-	66	155	5
Filament, Et-OH	7.0	-	69	156	12
Filament, Et-OH	9.8	-	70	156	12
Filament, Et-OH		4.5	77	158	30
P(L/DL)LA 70/30					
Granulate	-	-	60 – 62	121 - 122	14
Filament, Met-OH, L	1.4	-	62	-	-
Filament, Met-OH	7.0	-	65	-	-
Filament, Et-OH, L	1.4	-	62	-	-
Filament, Et-OH	7.0	-	64	-	-
Filament, Et-OH		3.0	60	114	1

The crystallinity of the P(L/D)LA 96/4 copolymer granulate was about 40%, T_m was 157°C and T_g in the range from 65 to 68°C. The wet-spun filaments had lower degrees of

crystallinities. The post-crystallization, that is cold-crystallization (X_{cc}) [Nelson *et al.* 2003; Cao *et al.* 2003; Solarski *et al.* 2005b], was observed with the wet-spun filaments. A peak temperature (T_{cc}) of cold-crystallization was observed slightly above T_g, as shown in Figure 15 on page 45, curve 2, 3, and 4. Very closely spaced T_g and cold-crystallization has been observed also in a stereocomplex type of 1:1 blend of P(L)LA and P(D)LA [Sarasua *et al.* 2005]. The initial degree of crystallinity (X) of 16% was calculated for the filaments coagulated either in methanol or ethanol, as shown in Table 9. The wet-spun filaments were more amorphous than the melt-spun filaments (X = 29%) which have been made from a similar copolymer [Ellä *et al.* 2007]. Spin drawing of wet-spun filaments was performed at room temperature under the T_g of copolymer, and thus crystallization of wet-spun filaments was induced only by orientation.

The longer coagulation time in ethanol increased the elongation at break (about 230 %), Table 10 on page 48, and the greater X_{cc} (17 %) was observed during the heating in DSC, as shown in Figure 15, curve 2. Hence, the initial crystallinity of the wet-spun filament was only 5%. Thus the longer coagulation time produced more amorphous P(L/D)LA 96/4 filaments. Crystallization of wet-spun filaments is low because solvent and non-solvent are present inside the filament when the intermolecular bonds begin to lock.

The T_m values of the P(L/D)LA 96/4 filaments remained practically unchanged when the spin draw ratio was increased from 1.4 to 9.8, as shown in Table 9. The lost of crystallinity was at maximum 4% when the spin draw ratio was increased from 1.4 to 9.8. Drawing orientates the filaments, and the crystals become thinner which can be seen as a decreased crystallinity [Gupta *et al.* 2006a; Turner *et al.* 2004]. The increase of the spin draw ratio from 1.4 to 9.8 increased T_g about 4°C with both coagulants, and the T_g was 70°C at the spin draw ratio of 9.8. The increase of the draw ratio increased the orientation of the amorphous zones and the number of intermolecular bonds, and this can be seen as an increasing T_g [Gupta *et al.* 2006a; Ellä *et al.* 2007]. The cold-crystallization started earlier when the spin draw ratio increased which can be seen as the decrease of the T_{cc}. It decreased about 7°C with the methanol coagulated filaments and about 5°C with ethanol coagulated filaments when the spin draw ratio increased from 1.4 to 9.8.

Hot drawing decreased the cold crystallization temperature and the cold crystallization enthalpy, see, Figure 15 curve 5 [Solarski *et al.* 2005b]. The crystallinity of hot-drawn filaments was higher (X = 30 %) than that of the as-spun and spin-drawn filaments, but it was not in the level of the original copolymer granulate. Hot drawing was conducted around the temperature of T_g, and crystallization was induced by temperature and orientation. This process is similar to melt spinning, and thus the crystallinity of hot-drawn filaments is more similar to melt-spun filaments. Compared to the melt-spun filaments [Ellä *et al.* 2007], the hot-drawn, wet-spun P(L/D)LA 96/4 filament had similar crystallinity. The increase of the T_g value was observed with the hot-drawn filaments. The T_g value was determined at 78ºC but the cold-crystallization peak was overlapped with the glass transition, see Figure 15 (curve 5).

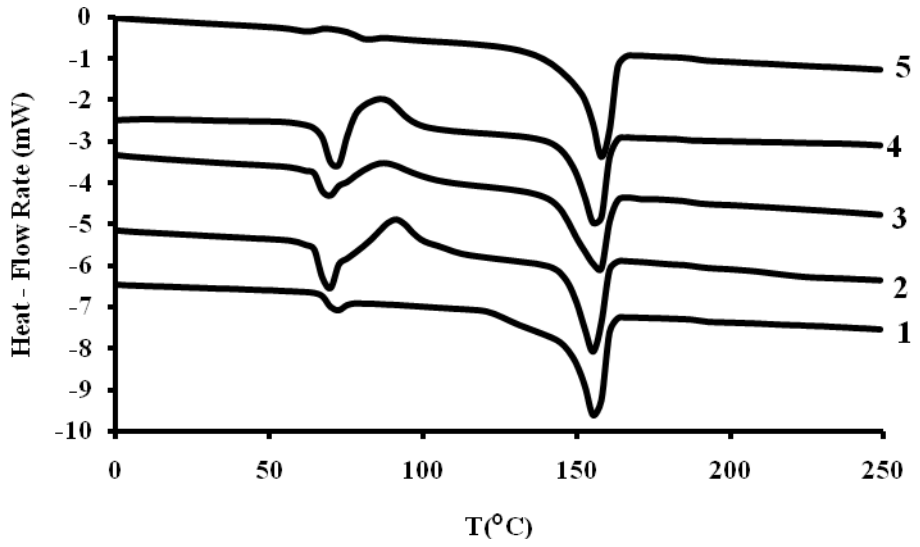

Figure 15 DSC-curves of P(L/D)LA 96/4: (1) granulate; (2) filament, spin draw ratio 1.4, long coagulation time, (3) filament, spin draw ratio 1.4, short coagulation time, (4) filament, spin draw ratio 7.0, and (5) filament, hot draw ratio 4.5; coagulant: ethanol.

The degree of crystallinity of the original partially crystalline P(L/DL)LA 70/30 granulates was about 14%, T_m was 122 °C, and T_g in the range from 60 to 62°C with an enthalpy relaxation (an endothermic peak) based on the DSC measurements, as shown in Table 9. The crystallinity of the P(L/DL)LA 70/30 filaments was lost and the filaments were amorphous, as shown in Figure 16. There was no cold-crystallization during the heating process of the P(L/DL)LA 70/30 filament in the DSC measurements. The

amorphous nature of the P(L/DL)LA 70/30 filaments did not change by increasing the spin draw ratio or by changing the coagulant, as shown in Table 9. Due to the presence of solvent and non-solvent in the filament structure during the coagulation process, the crystallization was not induced even with orientation.

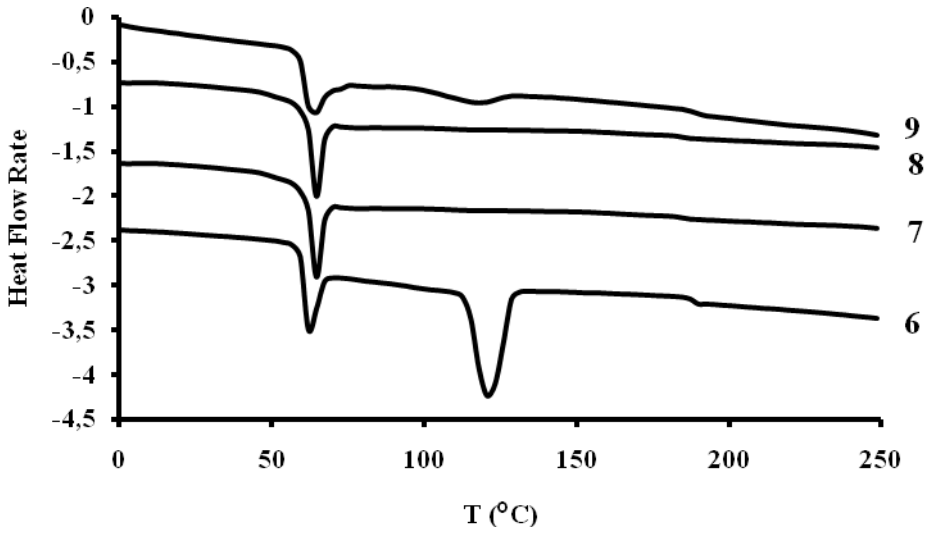

Figure 16 DSC-curves of P(L/DL)LA 70/30: (6) granulate, (7) filament, spin draw ratio 1.4, (8) filament, spin draw ratio 7.0, and (9) filament, hot draw ratio 3.0; coagulant: ethanol.

The hot-drawn P(L/DL)LA 70/30 filaments were also amorphous (X = 1%), as the spin-drawn P(L/DL)LA 70/30 filaments. Compared to the melt-spun P(L/DL)LA 70/30 filaments, the wet-spun, hot-drawn filaments had lower crystallinity [Fambri *et al.* 2006].

The drawing ability of the as-spun filaments can be explained by the thermal behaviour of the filaments. The better hot drawing ability of the as-spun P(L/D)LA 96/4 filament was caused by its higher T_g and T_m values. The as-spun P(L/DL)LA 70/30 filaments were amorphous and the shrinkability of the filaments was very high. This high shrinkability resisted the stretching of the filament yarn.

4.3.3 Mechanical Properties

The mechanical properties of wet-spun, spin-drawn filaments are studied in Paper II, those of hot-drawn filaments in Paper III, and those of protein-loaded filaments in Paper IV, respectively. The filament diameter was controllable by the draw ratio. It was possible to spin very fine filaments when the draw ratio was high. The diameters of the obtained wet-spun filaments were between 11 - 36 μm (1.0 – 7.5 dtex) as shown in Table 10. The methanol coagulated P(L/D)LA 96/4 filaments with the short coagulation time had larger diameter than other filaments manufactured by otherwise similar process parameters. Methanol is a smaller molecule than ethanol and it can diffuse easier into the polymer solution. The volume of methanol diffusing in was greater than the volume of dichloromethane diffusing out, and the filament solidified in the swollen state.

The diameters of the thinnest hot-drawn filaments were at the same level as the filaments prepared by the high spin draw ratio (9.8). Hot drawing stretched the filaments as spin drawing, and the filaments become thinner. The diameter of the hot-drawn P(L/D)LA 96/4 filament was as low as 14 μm (1.6 dtex) at the draw ratio of 4.5. Respectively, the diameter of the hot-drawn P(L,DL)LA filament was 15 μm (1.9 dtex) at the hot draw ratio of 3.0.

The protein-loaded filaments were thicker than the unloaded filaments. The mean diameter of the P(L/D)LA 96/4 filament was 46 μm (11 dtex) and that of the P(L/DL)LA 70/30 filament was 70 μm (19 dtex).

The multi-nozzle spinneret enabled the fabrication of the thin filaments compared to the syringe which has been used in the earlier studies. For example, the filaments with diameters between 28 – 550 μm have been produced by the wet spinning method [Nelson *et al.* 2003; Ngo *et al.* 2003], and by dry wet spinning the minimum diameter was about 50 μm [Gupta *et al.* 2006a]. The protein-loaded filaments fabricated by multi-nozzle spinneret in this study were as thin as or thinner than the drug-loaded filaments which were fabricated by the syringe in the other studies [Crow & Nelson 2006; Gao *et al.* 2007].

Table 10 Diameters, titers and mechanical properties of wet-spun filaments (SDR: spin draw ratio; HDR: hot draw ratio; S: short coagulation time; L: long coagulation time; P: protein-loaded).

SDR	*HDR*	*Diameter (μm)*	*Titer (dtex)*	*Tensile strength (cN/dtex)*	*Tensile strength (MPa)*	*Young's modulus (cN/dtex)*	*Young's modulus (GPa)*	*Elongation at break (%)*
Methanol coagulated P(L/D)LA 96/4								
1.4 S	-	36	7.5	0.7	49	10	0.7	92
7.0	-	18	2.1	1.1	90	13	1.0	67
9.8	-	14	1.3	1.1	94	15	1.3	47
Ethanol coagulated P(L/D)LA 96/4								
1.4 L	-	26	6.4	0.7	78	10	1.2	235
1.4 S	-	30	7.7	0.5	53	10	1.2	59
4.2	-	17	2.8	1.0	125	12	1.5	105
7.0	-	13	1.7	1.2	148	13	1.7	70
9.8	-	12	1.3	1.0	113	15	1.6	42
-	2.5	20	3.3	1.1	108	12	1.2	97
-	3.0	17	2.9	1.2	154	15	1.9	75
-	4.5	14	1.6	2.7	285	19	2.0	30
P	-	46	11	0.3	17	8	0.5	74
Methanol coagulated P(L/DL)LA 70/30								
1.4 L	-	29	5.6	0.5	45	9	0.8	231
4.2	--	17	2.1	1.2	103	11	1.0	94
7.0	-	13	1.3	1.5	148	13	1.3	59
9.8	-	11	1.0	1.3	126	14	1.3	41
Ethanol coagulated P(L/DL)LA 70/30								
1.4 L	-	27	5.5	0.6	56	9	0.9	211
4.2	-	18	2.1	1.3	105	11	0.9	82
7.0	-	14	1.4	1.6	146	14	1.3	47
9.8	-	12	1.0	1.5	135	14	1.3	34
-	2.0	17	2.5	1.3	130	14	1.5	69
-	3.0	15	1.9	1.6	175	12	1.3	44
P		70	19	0.2	7	7	0.4	62

The engineering stress values were also dependant on the draw ratio. The tensile strength values of spin-drawn P(L/D)LA 96/4 filaments were up to 150 MPa (1.2 cN/dtex) The highest tensile strength values were obtained at the spin draw ratio of 7.0. The increase of the spin draw ratio to 9.8 caused the overstretching of the molecular chains, and this can be seen as the decrease of tensile strength. The Young´s modulus value of the methanol coagulated spin-drawn P(L/D)LA 96/4 filaments was up to 1.3 GPa (15 cN/dtex) and that

of the ethanol coagulated spin-drawn filaments was up to 1.7 GPa (15 cN/dtex), as shown in Table 10. The coagulation conditions could have effect on the mechanical properties. The high efficient coagulant, as methanol in our study, can induce the high number of pores and capillaries inside the filament, and thus reduce the mechanical strength [Frushour & Knorr 2007].

Hot drawing, and thus temperature and orientation induced crystallization, increased the engineering stress values of the P(L/D)LA 96/4 filaments. The more crystalline hot-drawn filament had higher Young's modulus value compared to the lower crystalline spin-drawn filaments. The maximum Young's modulus value of the hot-drawn P(L/D)LA 96/4 filaments was 2.0 GPa (19 cN/dtex), and it was achieved at the hot draw ratio of 4.5. The tensile strength value of hot-drawn P(L/D)LA 96/4 filaments was 285 MPa (2.7 cN/dtex), and the filaments were as strong as commercial acrylic and viscose fibers manufactured by the wet spinning method [Haudek & Viti 1980, p. 47]. Hot drawing has caused strain hardening to polymer, and the stiffening and strengthening of polymer could be observed. During drawing the molecular chains slip past one another and become highly oriented.

The Young's modulus values of the spin-drawn P(L/DL)LA 70/30 filaments were up 1.3 GPa (14 cN/dtex) for both methanol and ethanol coagulated filaments, as shown in Table 10. The tensile strength values of spin-drawn P(L/DL)LA 70/30 filaments were up to 150 MPa (1.6 cN/dtex). These filaments were slightly less stiff as P(L/D)LA 96/4 filaments based on tensile modulus. This is caused by the amorphous nature of the spin-drawn P(L/DL)LA 70/30 filaments.

Hot drawing had not such a positive effect on the engineering stress values of P(L/DL)LA 70/30 filaments as with P(L/D)LA 96/4. Hot drawing increased only slightly the degree of crystallinity, and thus the stress values have been improved only slightly compared to spin-drawn filaments. The maximum tensile strength of the hot-drawn P(L/DL)LA 70/30 filament was 175 MPa (1.6 cN/dtex) and Young's modulus was 1.5 GPa (14 cN/dtex). The maximum tensile strength value of the hot-drawn P(L/DL)LA 70/30 filaments is at the same level as the values of commercial triacetate and acetate fibres [Haudek & Viti 1980, p. 47].

The mechanical properties of the protein-loaded filaments were much lower than those of unloaded filaments. The tensile strength of the protein-loaded P(L/D)LA 96/4 filament was 17 MPa (0.3 cN/dtex) and that of the P(L/DL)LA 70/30 filament was only 7 MPa (0.2 cN/dtex). The Young's modulus value was 0.5 GPa (8 cN/dtex) for the protein-loaded P(L/D)LA 96/4 filament and 0.4 GPa (7 cN/dtex) for the protein-loaded P(L/DL)LA 70/30 filament. The low mechanical properties are caused by a high number of large pores inside the filaments.

The coagulation time had effect on the elongation at break of filaments. In this study two different coagulation times were tested at the spin draw ratio of 1.4 and with methanol coagulant. The long coagulation time (5.6 s) ensured the long elongation at break (more than 200 %). If the coagulation time was short (1.9 s) at the same spin draw ratio, the elongation at break values were lower (59 – 105 %). The filaments with the short coagulation time had also higher degree of crystallinity. The elongation of the as-spun filament has importance, for example, in a separate hot drawing. The high elongation at break value enables high draw ratios in hot drawing.

The stress-strain curves of the P(L/D)LA 96/4 filaments are presented in Figure 17 and those of the P(L/DL)LA 70/30 filaments in Figure 18.

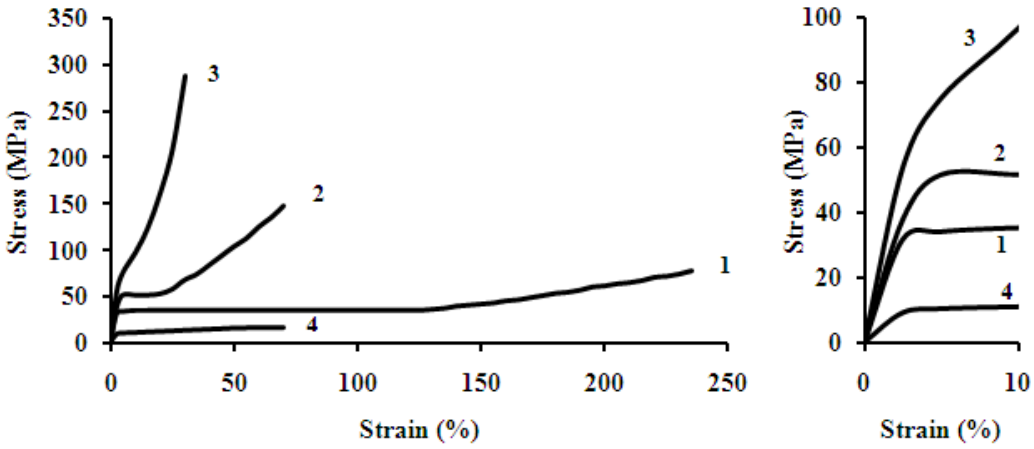

Figure 17 Engineering stress-strain curves of P(L/D)LA 96/4 filaments: (1) spin draw ratio 1.4 (as-spun); (2) spin draw ratio 7.0; (3) hot draw ratio 4.5; and (4) protein-loaded. Coagulant: ethanol. Curves on the right show details from the beginning of the curves on the left.

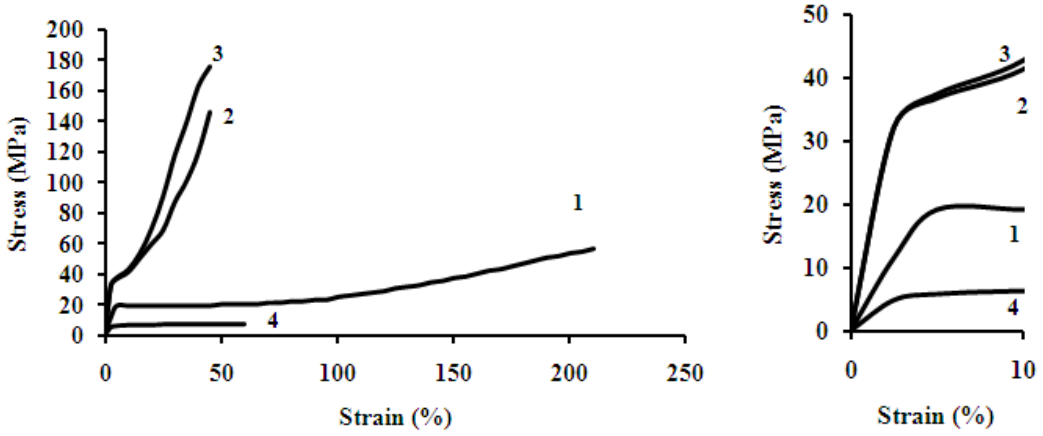

Figure 18 Engineering stress-strain curves of P(L/DL)LA 70/30 filaments: (1) spin draw ratio 1.4 (as-spun); (2) spin draw ratio 7.0; (3) hot draw ratio 3.0; and (4) protein-loaded. Coagulant: ethanol. Curves on the right show details from the beginning of the curves on the left.

As conclusions, both as-spun filaments had very high elongation at break and low Young's modulus values which describe that they were easily drawable. Spin drawing increased the alignment of polymer chains, but because of drawing at room temperature, it increased very slightly or not at all the degree of crystallinity. Hot drawing also increased the alignment of polymer chains. The raised temperature increased the temperature induced crystallinity of P(L/D)LA 96/4, and this can be observed as increased stiffness. The raised temperature did not increased the degree of crystallinity of P(L/DL)LA 70/30, and the stiffness of spin-drawn and hot-drawn P(L/DL)LA 70/30 was similar.

4.3.4 *In Vitro* Degradation of Filaments

The *in vitro* degradation of the spin-drawn filaments are studied in Paper II, that of the hot-drawn filaments in Paper III, and that of the protein-loaded filaments in Paper IV, respectively. In this summary the *in vitro* hydrolytic degradation results are calculated from the cN/dtex –results, whereas the results in Papers II and III are calculated from the MPa –values. In cN/dtex –values have been used the wet, swollen titer values, whereas in MPa –values the diameters of the dry filaments. The retention of tensile strength of the spin-drawn P(L/D)LA 96/4 filaments are presented in Figure 19. The tested filament was

spun at the low spin draw ratio and the coagulation time was short (1.9 s). Those spinning parameters gave about 16% crystallinity to the P(L/D)LA 96/4 filaments. After 16 weeks *in vitro* the filaments had left about 80 - 85% from their initial tensile strength and after 52 weeks *in vitro* about 45% had left from their initial tensile strength.

The degree of crystallinity has influence on the degradation properties of polylactide. During the hydrolytic degradation water diffuses into the amorphous regions of polymer and causes the breakage of the ester bonds which initiates a reduction in molar mass and later on a reduction in mechanical strength. After amorphous regions the hydrolytic degradation occurs in the crystalline regions leading to increased mass loss and finally to complete desorption. [Vert *et al.* 1992]

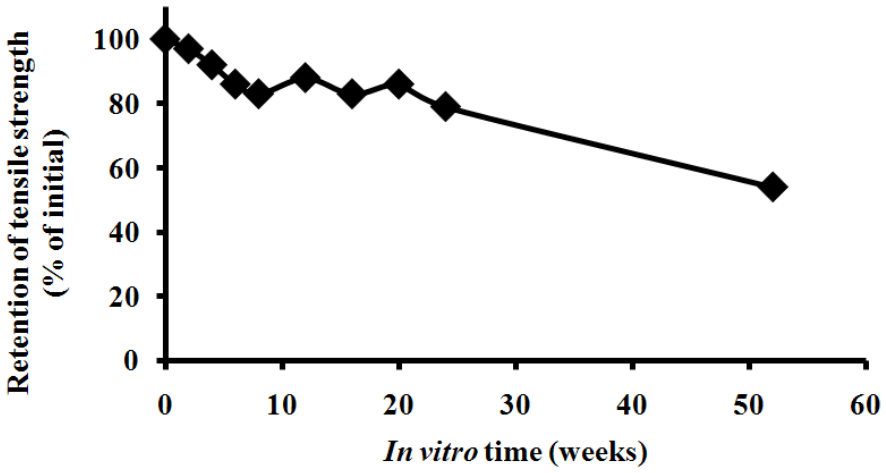

Figure 19 *In vitro* retention of P(L/DL)LA 96/4 filament; spin draw ratio 1.4; short coagulation time; coagulant: methanol.

The *in vitro* hydrolytic degradation results of the spin-drawn and the hot-drawn P(L/DL)LA 70/30 filaments are presented in Figure 20. The as-spun and the spin-drawn filaments were totally amorphous and the hot-drawn filaments were also practically amorphous (X = 1%). The as-spun and the spin-drawn filaments had left about 30% from their initial tensile strength after 16 weeks *in vitro*. After this period the filaments broke when they were pinched between the tensile tester clamps, and the tenacity results were not any more reliable. Thus, the degradation rate of the P(L/DL)LA 70/30 filaments was faster than that of the P(L/D)LA 96/4 filaments. Because the P(L/DL)LA 70/30 filaments were amorphous, water was able to penetrate more easily into the filament structure.

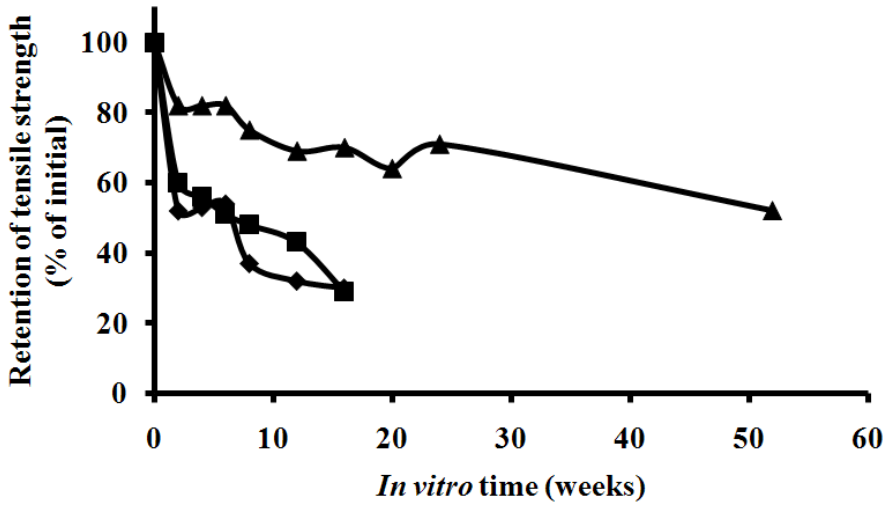

Figure 20 *In vitro* retention of P(L/DL)LA 70/30 filament: (▲) hot-drawn filament at hot draw ratio of 3.0, (■) as-spun filament, and (♦) spin-drawn filament at spin draw ratio of 7.0; coagulant: ethanol.

Hot drawing decreased the *in vitro* degradation rate of the P(L/DL)LA 70/30 filaments. After 16 weeks *in vitro* the hot-drawn P(L/DL)LA 70/30 filaments had left about 70 % from their initial tenacity, and after 52 weeks about 50 % from their initial tenacity. Despite the hot-drawn P(L/DL)LA 70/30 filaments were also practically amorphous, their degradation rate was slower than that of the spin-drawn filaments having similar diameter. Probably hot drawing had effect on the filament structure, and water was not able to penetrate into the filament structure as easily as into the spin-drawn filaments.

The degradation rate of the polylactide stereo copolymers is faster than that of enantiomerically pure polylactide. The degradation of semi-crystalline self-reinforced (SR) P(L)LA plates (X = 53 %) could take many years [Suuronen *et al.* 1998]. After five years *in vivo*, small particles of polymers still existed, but the mechanical strength of material was lost. The *in vitro* hydrolytic degradation of melt-spun P(L/D)LA 96/4 filaments was slower compared to the wet-spun filaments [Paakinaho *et al.* 2009]. The tenacity loss of the melt-spun filaments has been about 11 % after 24 weeks *in vitro*. The melt-spun filaments have been γ-irradiated (25 kGy) for sterility, and the results are not fully comparable. Totally amorphous SR P(L/DL)LA 70/30 screws have had cracks, clefts and fragmentation after 24 weeks *in vivo* [Kallela *et al.* 1999]. Under *in vitro* hydrolysis the material lost its mechanical strength after 48 weeks.

The mechanical properties of protein-loaded filaments were not measured during *in vitro* testing. However, after 16 weeks *in vitro* the mechanical strength of the protein-loaded P(L/DL)LA 70/30 filaments was so low that the filaments started to broke, and there were short filaments in the test tube as in the *in vitro* study of the spin-drawn P(L/DL)LA 70/30 filaments.

The SEM-images of the protein-loaded filaments after 24 weeks *in vitro* are presented in Figure 21. After this period it was observed a distinct erosion in the cross-section of the P(L/DL)LA 70/30 filament, whereas it was not so clear with the P(L/D)LA 96/4 filament. Li and co-workers [1990] have noticed more rapid degradation in the centre of amorphous specimen than at the surface of it. They have suggested that amorphous polylactide specimen has absorbed the aqueous medium and the breakages of ester bonds have started from the centre, and the specimen have become hollow gradually. The acid degradation products of polylactide can cause autocatalytic effects leading to faster erosion inside the specimen compared to the surface [Göpferich 1997]. On the other hand, a regular pattern of cracks along the vertical direction of the semicrystalline P(L)LA filament has been observed [Nishimura *et al.* 2005; Gupta *et al.* 2007a].

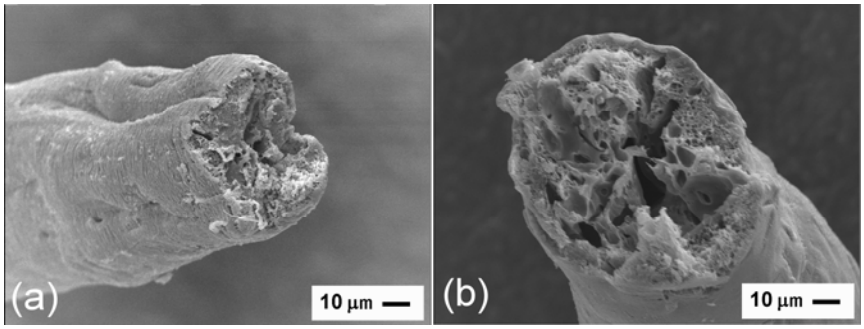

Figure 21 SEM-images of protein-loaded filaments after 24 weeks *in vitro*: (a) P(L/D)LA 96/4 and (b) P(L/DL)LA 70/30.

The cumulative BSA release curve of the protein-loaded P(L/D)LA 96/4 filament is presented in Figure 22 and that of the protein-loaded P(L/DL)LA 70/30 filament in Figure 23. The burst effect can be observed in the beginning of both curves. During this period the protein molecules from the surface were released to the soaking solution. After this period the release of BSA was slower because the soaking solution had not yet effected

on the filament polymer. The BSA release of the P(L/DL)LA 70/30 filament was slightly accelerated after 9 weeks, whereas this was not observed with the P(L/D)LA 96/4 filament. The total amount of the released BSA was higher with the P(L/DL)LA 70/30 filament.

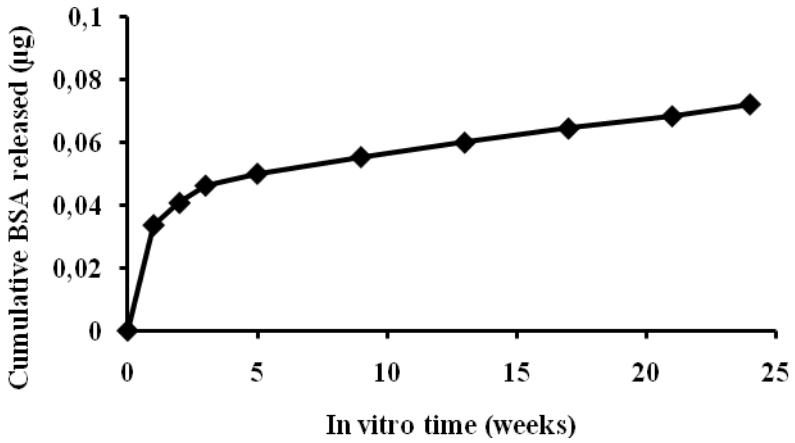

Figure 22 *In vitro* cumulative BSA released from the protein-loaded P(L/D)LA 96/4 filaments.

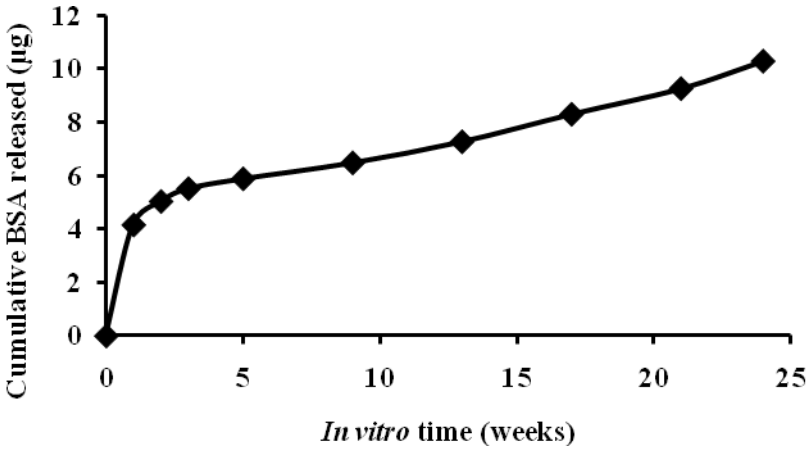

Figure 23 *In vitro* cumulative BSA released from the protein-loaded P(L/DL)LA 70/30 filament.

The drug release rate is determined by the degradation time of polymer and the diffusion of drug molecule. Because polylactide is a hydrophobic polymer its degradation rate is slower than that of hydrophilic polymers. Hydrophilic polymer swells easily in aqueous media, and the release of drug from swollen polymer is easier. [Kwon & Furgeson 2007]

BSA is a single polypeptide chain, and its molecular weight was about 66 500 according to the supplier. It is a big molecule, and thus the diffusion of BSA from the polymer matrix is slow.

The release of ciprofloxacin (CF) from screws made from SR P(L/DL)LA 70/30 have been studied, and the increasing concentrations of CF after 9 weeks *in vitro* have been observed [Veiranto *et al.* 2002]. CF has been totally released after 44 weeks *in vitro*. The theoretical release time of 44 weeks is a too long time in many purposes, like in tissue engineering. For example, shorter release time has been observed with poly(DL-lactide-co-glycolide) (PDLGA). Totally 6 weeks release time of protein has been measured for thin microspheres made from the low molecular weight PDLGA [Zilberman *et al.* 2004].

5 CONCLUSIONS

This work described the wet spinning method of polylactide stereo copolymer filaments for the laboratory or small-scale manufacturing. It also presented the effect of spin drawing, hot drawing, and protein loading on the properties of wet-spun filaments.

Dichloromethane was chosen from the analyzed polymer solvents because it dissolved both P(L/D)LA 96/4 and P(L/DL)LA 70/30. Respectively, methanol and ethanol were chosen from the analyzed non-solvents for the spinning trials. Their precipitation properties were quite similar and their use in the laboratory-scale was easy.

Spin drawing orientated the polymer chains without the elevated temperature. The maximum mechanical strength was achieved at the spin draw rate of 7.0 with both polymers. The further drawing decreased the tensile strength because of overstretching of polymer chains. The diameters of filaments were about 13 – 18 μm at this spin draw ratio using the tested spin dope concentration and spinneret configuration. If thinner diameters are wanted, the lower spin dope concentrations, the decreased pump capacity, or the decreased hole diameter are possible to use.

Hot drawing increased especially the tensile strength of P(L/D)LA 96/4 filament (285 MPa; 2.7 cN/dtex) compared to spin drawing, and hot drawing also increased the degree of crystallinity of the filament. Hot drawing declined the *in vitro* degradation rate of filaments made from both polymers, despite it did not practically increased the degree of crystallinity of P(L/DL)LA 70/30 filaments.

Because the wet spinning method do not need elevated temperature it is possible to add heat sensitive drugs, as proteins, to the spin dope. The spin dope of the protein-loaded filaments was made by probe sonication of polymer and protein solution. Probe sonication created air bubbles to the spin dope, and they were observed as large pores inside the filaments. It also significantly reduced the tensile strength of filaments. The *in vitro* release rate of protein was slow due to the degradation rate of polymer and the size of protein.

Spin drawing is recommendable choice for manufacturing of wet-spun polylactide stereo copolymer filaments if very thin filaments or short degradation rate is wanted. On the other hand, hot-drawing is advisable aftertreatment of filaments if higher tensile strength is needed.

Because the filaments were manufactured from the medical grade polymers, they are possible to use in the medical end-uses where the moderate mechanical strength is sufficient. One example of end-uses is non-woven scaffolds for tissue engineering.

REFERENCES

Agrawal, A., Amid, D.S., Rath, S.S. & Khanna, A. 2004. Constrained nonlinear optimization for solubility parameters of poly(lactic acid) and poly(glycolic acid) – validation and comparison. Polymer 45, pp. 8603-8612.

Auras, R., Harte, B. & Selke, S. 2004. An overview of polylactides as packaging materials. Macromolecular Bioscience 4, pp. 835-864.

Bezemer, J.M., van Blitterswijk, C.A., Feijen, J. & Grijpma, D.W. 2004. Preparation of fibrous polymer implant containing bioactive agents using wet spinning technique. US Patent 6,685,957.

Blomqvist, J., Mannfors, B. & Pietilä, L.-O. 2002. Amorphous cell studies of polyglycolic, poly(L-lactid), poly(L,D-lactic) and poly(glycolic/L-lactic) acids. Polymer 43, pp. 4571-4583.

Cao, X, Mohamed, A., Gordon, S.H., Willett, J.L. & Sessa, D.J. 2003. DSC study of biodegradable poly(lactic acid) and poly(hydroxy ester ether) blends. Thermochimica Acta 406, pp. 115-127.

Cartier, L., Okihara, T., Ikada, Y., Tsuji, H., Puiggali, J. & Lotz, B., 2000. Epitaxial crystallization and crystalline polymorphism of polylactides. Polymer 41, pp. 8909-8919.

Chen, J., Wang, C., Dong, X. & Liu, H. 2006. Study on the coagulation mechanism of wet-spinning PAN fibers. Journal of Polymer Research 13, pp. 515-519.

Cicero, J.A. & Dorgan, J.R. 2001. Physical properties and fiber morphology of poly(lactic acid) obtained from continuous two-step melt spinning. Journal of Polymers and the Environment 9, pp. 1-10.

CIRFS 2010. Statistical Yearbook 2010. Information on Man-Made Fibers. Bruxelles, Comité International de la Rayonne et des Fibres Synthétiques. 278 p.

Crow, B.B., Borneman, A.F., Hawkins, D.L., Smith, G.M. & Nelson, K.D. 2005. Evaluation of *in vitro* drug release, pH change, and molecular weight degradation of poly(L-lactic acid) and poly(D,L-lactide-co-glycolide) fibers. Tissue Engineering 11, pp. 1077-1084.

Crow, B.B. & Nelson, K.D. 2006. Release of bovine serum albumin from a hydrogel-cored biodegradable polymer fiber. Biopolymers 81, pp. 419-427.

Denkbas, E.B., Seyyal, M. & Piskin, E. 2000. Implantable 5-fluorouracil loaded chitosan scaffolds prepared by wet spinning. Journal of Membrane Science 172, pp. 33-38.

Eling, B., Gogolewski, S. & Pennings, A.J., 1982. Biodegradable materials of poly(L-lactic acid) I. Melt-spun and solution-spun fibres. Polymer 23, pp. 1587-1593.

Ellä, V., Kellomäki, M. & Törmälä, P. 2005. In vitro properties of PLLA screws and novel bioabsorbable implant with elastic nucleus to replace intervertebral disc. Journal of Materials Science: Materials in Medicine 16, pp. 655-662.

Ellä, V., Gomes, M.E., Reis, R.L., Törmälä, P. & Kellomäki, M. 2007. Studies of P(L/D)LA 96/4 non-woven scaffolds and fibres; properties, wettability and cell spreading before and after intrusive treatment methods. Journal of Materials Science: Materials in Medicine 18, pp. 1253-1261.

Eppley, B.L. 2003. Use of resorbable and screw fixation in pediatric craniofacial surgery. Operative Techniques in Plastic and Reconstructive Surgery 9, pp. 36-45.

Fambri, L., Pegoretti, A., Mazzurana, M. & Migliaresi, C. 1994. Biodegradable fibers Part I Poly-L-lactic acid fibres produced by solution spinning. Journal of materials science: Materials in medicine 5, pp. 679-683.

Fambri, L, Pegoretti, A., Fenner, R., Incardona, S.D. & Migliaresi, C. 1997. Biodegradable fibres of poly(L-lactic acid) produced by melt spinning. Polymer 38, pp. 79-85.

Fambri, L., Bragagna, S. & Migliaresi, C. 2006. Biodegradable fibers of poly-L,DL-lactide 70/30 produced by melt spinning. Macromolecular symposia 234, pp. 20-25.

Ferguson, S., Wahl, D. & Gogolewski, S. 1996. Enhancement of the mechanical properties of polylactides by solid-state extrusion. II. Poly(L-lactide), poly(L/D-lactide), and poly(L/DL-lactide). Journal of Biomedical Materials Research, Part A 30, pp. 543-551.

Fischer, E.W., Sterzel, H. J. & Wegner, G. 1973. Investigation of the structure of solution grown crystals of lactide copolymers by means of chemical reactions. Kolloid-Zeitschrift & Zeitschrift für Polymere 251, pp. 980-990.

Freeman, J.W., Wright, L.D., Laurencin, C.T. & Bhattacharyya, S. 2008. Nanofabrication Techniques. In: Gonsalves, K.E., Halberstadt, C.R., Laurencin, C.T., Nair, L.S (ed.). Biomedical Nanostructures, Hoboken, USA, John Wiley & Sons Inc. pp. 3-24.

Fritzsche, H., Rupprecht, A. & Richter, M. 1984. Infrared linear dichroism of oriented DNA-ligand complexes prepared with the wet-spinning method. Nucleic Acid Research 12, pp. 9165-9177.

Fourne, F. 1999. Synthetic Fibers – Machines and Equipment, Manufacture, Properties. Munich, Germany, Hanser Publishers. 930 p.

Frushour, B.G. & Knorr, R.S. 2007. Acrylic Fibers. In: Lewin, M. (ed.). Handbook of Fiber Chemistry, 3. ed. Boca Raton, USA, CRC Press, pp. 811-974.

Furuhashi, Y., Kimura, Y., Yoshie, N. & Yamane, H. 2006. Higher-order structures and mechanical properties of stereocomplex-type poly(lactic acid) melt spun fibers. Polymer 47, pp. 5965-5972.

Furuhashi, Y., Kimura, Y. & Yamane, H. 2007. Higher Order Structural Analysis of Stereocomplex-Type Poly(lactic acid) Melt-Spun Fibers. Journal of Polymer Science: Part B: Polymer Physics 45, pp. 218-228.

Gao, H., Gu, Y. & Ping, Q. 2007. The implantable 5-fluorouracil-loaded poly(L-lactic acid) fibers prepared by wet-spinning from suspension. Journal of Controlled Release 118, pp. 325-332.

Ghosh, S. & Vasanthan, N. 2006. Structure development of poly(L-lactic acid) fibers processed at various spinning conditions. Journal of Applied Polymer Science 101, pp. 1210-1216.

Greidanus, P.J., Feijen, J., Eenink, M.J.D., Rieke, J.C., Olijslager, J. & Albers, J.H.M. 1990. Biodegradable polymer substrates loaded with active substance suitable for the controlled release of the active substance by means of a membrane. US Patent 4,965,128.

Gogolewski, S. & Pennings A.J. 1983. Resorbable materials of poly(L-Lactide). II. Fibers spun from solutions of poly(L-Lactide) in good solvents. Journal of Applied Polymer Science 28, pp 1045-1061.

Gupta, B. Revagade, N., Anjum, N., Atthoff, B. & Hilborn, J. 2006a. Preparation of poly(lactic acid) fiber by dry-jet-wet-spinning. I. Influence of draw ratio on fiber properties. Journal of Applied Polymer Science 100, pp. 1239-1246.

Gupta, B. Revagade, N., Anjum, N., Atthoff, B. & Hilborn, J. 2006b. Preparation of poly(lactic acid) fiber by dry-jet-wet-spinning. II. Effect of process parameters on fiber properties. Journal of Applied Polymer Science 101, pp. 3774-3780.

Gupta, B., Revagade, N. & Hilborn, J. 2007a. In vitro degradation of dry-jet-wet-spun poly(lactic acid) monofilament and knitted scaffold, Journal of Applied Polymer Science 103, pp. 2006-2012.

Gupta, B., Revagade, N. & Hilborn, J. 2007b. Poly(lactic acid) fiber: An overview. Progress in Polymer Science 32, pp. 455-482.

Göpferich, A. 1997. Mechanisms of polymer degradation and elimination. In: Domb, J. A., Kost, J. & Wiseman, D. M. (ed.). Drug Targeting and Delivery. Vol. 7: Handbook of Biodegradable Polymers. Boca Raton, USA, CRC Press.

Götze, K. 1967. Chemiefasern nach dem viskosverfahren, Erster Band, 3. Auflage, Berlin, Germany, Springer-Verlag. p. 778.

Hansen, C.M. 2000. Hansen Solubility Parameters, A Users's Handbook. Boca Raton, USA, CRC Press.

Haudek, H.W. & Viti, E. 1980. Textilfasern. Wien, Germany, Verlag Johann L. Bondi & Sohn. 361 p.

Hausberger, A.G. & DeLuca, P.P. 1995. Characterization of biodegradable poly(D,L-lactide-co-glycolide) polymers and microspheres. Journal of Pharmaceutical & Biomedical Analysis 13, pp. 747-760.

He, C.-L., Huang, Z.-M., Han, X.-J., Liu, L., Zhang, H.-S. & Chen, L.-S. 2006. Coaxial electrospun poly(L-lactic acid) ultrafine fibers for sustained drug delivery. Journal of Macromolecular Science, Part B: Physics 45 pp. 515-524.

Hoogsten, W., Postema, A.R., Pennings, A.J., Brinke G. & Zugenmair, P. 1990. Crystal structure, conformation and morphology of solution-spun poly(L-lactide) fibers. Macromolecules 23, pp. 634-642.

Horáček, I. & Kalíšek, V. 1994a. Polylactide. I. Continuous dry spinning – hot drawing preparation of fibers. Journal of Applied Polymer Science 54, pp. 1751-1757.

Horáček, I. & Kalíšek, V. 1994b. Polylactide. II. Discontinuous dry spinning – hot drawing preparation of fibers. Journal of Applied Polymer Science 54, pp. 1759-1765.

Horáček, I. & Kalíšek, V. 1994c. Polylactide. III. Fiber preparation by spinning in precipitant vapor. Journal of Applied Polymer Science 54, pp. 1767-1771.

Houis, S., Schreiber, F. & Gries, Th. 2008. Bicomponent fibers (Part 1). Chemical Fibers International 58, pp.38-45.

Huang, S. J. 2005. Poly(lactic Acid) and copolyesters. In: Bastioli, C. (ed.). Handbook of Biodegradable Polymers. Shropshire, UK, Smithers Rapra. pp. 287-302.

Hussain, M.A., DiLuccio, R.C., Shefter, E. & Hurwitz, A.R. 1989. Hollow fibers as an oral sustained-release delivery system using propranolol hydrochloride. Pharmaceutical Research 6, pp. 1052-1055.

Ikada, Y. & Gen, S. 1991. Polylactic acid fiber. US Patent 5,010,145.

Johnson, R.M., Mwaikambo, L.Y. & Tucker, N. 2003. Biopolymers. In: Humpreys, S. (ed.). Rapra Review Reports. Vol. 14, Report 159. Shropshire, UK. Smithers Rapra. 143 p.

Kallela, I., Tulamo, R.-M., Hietanen, J., Pohjonen, T. & Suuronen, R. 1999. Fixation of mandibular body osteotomics using biodegradable amorphous self-reinforced (70L:30DL) polylactide or metal lag screws: an experimental study in sheep. Journal of Cranio-Maxillofacial Surgery 27, pp. 124-133.

Kellomäki, M., Pohjonen, T. & Törmälä, P. 2003. Self Reinforced Polylactides. In: Arshady, R. (ed.). The PBM Series. Vol. 2. London, UK, Citus Books, pp. 212-235.

Kulkarni, R.K., Pani, K.C. Neuman, C. & Leonard, F. 1966. Polylactic acid for surgical implants. Archives of Surgery 93, pp. 839-843.

Kwon, G.S. & Furgeson, D.Y. 2007. Biodegradable polymers for drug delivery systems. In: Jenkins, M. (ed.). Biomedical polymers. Cambridge, UK, Woodhead Publishing. pp. 83-110.

LaNieve, H.L. 2007. Cellulose Acetate and Triacetate Fibers. In: Lewin, M. (ed.). Handbook of Fiber Chemistry, 3. ed. Boca Raton, USA, CRC Press. pp. 773-810.

Lazzeri, L., Cascone, M.G., Quiriconi, S., Morabito, L. & Giusti, P. 2005. Biodegradable hollow microfibres to produce bioactive scaffolds. Polymer International 54, pp. 101-107.

Leenslag, J.W. & Pennings, A.J. 1987. High-strength poly(L-lactide) fibres by a dry-spinning/hot-drawing process. Polymer 28, pp. 1695-1702.

Li, D. & Xia, Y. 2004. Electrospinning of nanofibers: reinventing the wheel? Advanced Materials 16, pp. 1151-1169.

Li, D., Frey, M.W. & Baeumner, A.J. 2006 Electrospun polylactic acid nanofiber membranes as substrates for biosensor assemblies. Journal of Membrane Science 279, pp. 354-363.

Li, S. M., Garreau, H. & Vert, M. 1990. Structure-property relationships in the case of the degradation of massive aliphatic poly-(α-hydroxy acids) in aqueous media, Part 1: Poly(DL-lactic acid). Journal of Materials Science: Materials in Medicine 1, pp. 123-130.

Linnemann, B., Sri Harwoko, M. & Gries, Th., 2003. Polylactide fibers (PLA). Chemical Fibers International 53, pp. 426-433.

Maurus, P.B. & Kaeding, C.C. 2004. Bioabsorbable implant material review. Operative Techniques in Sports Medicine 12, pp. 158-160.

Mezghani, K. & Spruiell, J. E. 1998. High speed melt spinning of poly(L-lactic acid) filaments. Journal of Polymer Science 36, pp. 1005-1012.

Miraftab, M., Qiao, Q., Kennedy, J.F., Anand, S.C. & Groocock, M.R. 2003. Fibres for wound dressings based on mixed carbohydrate polymer fibres. Carbohydrate Polymers 53, pp. 225-231.

Morton, W.E. & Hearle, J.W.S. 1997. Physical Properties of Textile Fibres. Manchester, UK, The Textile Institute. 725 p.

Murakami, H., Kobayashi, M., Takeuchi, H. & Kawashima, Y. 2000. Further application of a modified spontaneous emulsification solvent diffusion method to various types of PLGA and PLA polymers for preparation of nanoparticles. Powder Technology 107, pp. 137-143.

Ndreu, A, Nikkola, L., Ylikauppila, H., Ashammakhi, N. & Hasirci, V. 2008. Electrospun biodegradable nanofibrous mats for tissue engineering. Nanomedicine 3, pp. 45-60.

Ngo, T.-T.B., Waggoner, P.J., Romero, A.A., Nelson, K. ., Eberhart, R.C. & Smith, G.M. 2003. Poly(L-Lactide) microfilaments enhance peripheral nerve regeneration across extended nerve lesions. Journal of neuroscience research 72, pp. 227-238.

Nelson, K.D., Romero, A., Waggoner, P., Crow, B., Borneman, A. & Smith, G. M. 2003. Technique paper for wet-Spinning poly(L-lactic acid) and poly(DL-lactide-co-glycolide) monofilament fibers. Tissue Engineering 9, pp. 1323-1330.

Nelson, K.D. & Crow. B.B. 2006. Drug releasing biodegradable fiber for delivery of therapeutics. US Patent 7,033,603.

Nishimura, Y., Takasu, A., Inai, Y. & Hirabayashi, T. 2005. Melt Spinning of poly(L-lactic acid) and its biodegradability. Journal of Applied Polymer Science 97, pp. 2118-2124.

Ogata, N., Yamaguchi, S., Shimada, N., Lu, G., Iwata, T., Nakane, K. & Ogihara, T. 2006. Poly(lactide) nanofibers produced by melt-electrospinning system with a laser melting device. Journal of Applied Polymer Science 104, pp. 1640-1645.

Paakinaho, K., Ellä, V., Syrjälä, S. & Kellomäki, M. 2009. Melt spinning of poly(L/D)lactide 96/4: Effect of molecular weight and melt processing on hydrolytic degradation. Polymer Degradation and Stability 94, pp. 438-442.

Penning, J.P., Dijkstra, H. & Pennings, A.J. 1993. Preparation and properties of absorbable fibres from L-lactide copolymers. Polymer 34, pp. 942-951.

Perepelkin, K.E. 2002. Chemistry and technology of chemical fibres Polylactide fibres: fabrication, properties, use, prospects. A review. Fibre Chemistry 34, pp. 85-100.

Perrin, D.E. & English, J.P. 1997. Polyglycolide and polylactide. In: Domb, J. A., Kost, J. & Wiseman, D. M. (ed.). Drug Targeting and Delivery. Vol. 7: Handbook of Biodegradable Polymers. Boca Raton, USA, CRC Press.

Park, C.H., Hong, E.Y. & Kang, Y.K. 2007. Effects of spinning speed and heat treatment on the mechanical properties and biodegradability of poly(lactic acid) fibers. Journal of Applied Polymer Science 103, pp. 3099-3104**.**

Polacco, G., Cascone, M.G., Lazzeri, L., Ferrara, S. & Giusti, P. 2002. Biodegradable hollow fibres containing drug-loaded nanoparticles as controlled release systems. Polymer International 51, pp. 1464-1472.

Postema, A.R. & Pennings, A.J. 1989. Study on the drawing behavior of poly(L-lactide) to obtain high-strength fibers. Journal of Applied Polymer Science 37, pp. 2351-2369.

Postema, A.R., Luiten, A.H. & Pennings, A.J. 1990a. High-strength poly(L-lactide) fibers by a dry-spinning / hot-drawing process. I. Influence of the ambient temperature on the dry-spinning process. Journal of Applied Polymer Science 39, pp. 1265-1274.

Postema, A.R., Luiten, A.H., Oostra, H. & Pennings, A.J. 1990b. High-strength poly(L-lactide) fibers by a dry-spinning / hot-drawing Process. II. Influence of the extrusion speed and winding speed on the dry-spinning process. Journal of applied polymer science 39, pp. 1275-1288.

Sarasua, J.-R., Rodrígues, N.L., Arraiza, A.L. & Meaurio, E. 2005. Stereoselctive crystallization and Specific Interactions in Polylactides. Macromolecules 38, pp. 8362-8371.

Schenderlein, S., Lück, M. & Müller, B.W. 2004. Partial solubility parameters of poly(D,L-lactide-co-glycolide). International Journal of Pharmaceutics 286, pp. 19-26.

Schmack, G., Tändler, B., Vogel, R., Beyreuther, R., Jacobsen, S. & Fritz, H.-G. 1999. Biodegradable fibers of poly(L-lactide) produced by high-speed melt spinning and spin drawing. Journal of Applied Polymer Science 73, pp. 2785-2797.

Schmack, G, Tändler, B., Optiz, G., Vogel, R., Komber, H., Häußler, L., Voigt, D., Weinmann, S., Heinemann, M. & Fritz, H.-G. 2004. High-speed melt spinning of various grades of polylactides. Journal of Applied Polymer Science 91, pp. 800-806.

Shah, S.S., Cha, Y. & Pitt, C.G. 1992. Poly(glycolic acid-co-DL-lactic acid): diffusion or degradation controlled drug delivery? Journal of Controlled Release 18, pp. 261-270.

Schindler, W.D. & Hauser, P.J. 2004. Chemical finishing of textiles. Boca Raton, USA, CRC Press. 213 p.

Solarski, S., Ferreira, M. & Devaux, E. 2005a. Influence of draw roll temperature on thermal and tensile properties of PLA filaments produced by melt spinning. Chemical Fibers International 55, pp. 180-182.

Solarski, S., Ferreira, M. & Devaux, E. 2005b. Characterization of the thermal properties of PLA fibers by modulated differential scanning calorimetry. Polymer 46, pp. 11187-11192.

Spruiell, J. E. & Bond, E. 1999. Melt spinning of polypropylene. In: Karger-Kocsis, J. (ed.). Polypropylene An A – Z reference. Dordrecht, The Netherlands, Kluwer Academic Publishers. pp. 427-445.

Stack, R. S., Clark, H. G., Walker, W. F. & McElhaney, J. H. 1996. Bioabsorbable stent and method of making the same. US Patent 5,527,337.

Suuronen, R., Pohjonen, T., Hietanen, J. & Lindqvist, C. 1998. A 5-year in vitro and in vivo study of the biodegradation of polylactide plates. Journal of Oral and Maxillofacial Surgery 56, pp. 604-614.

Södergård, A. & Stolt, M. 2002. Properties of lactic acid based polymers and their correlation with composition. Progress in Polymer Science 27, pp. 1123-1163.

Takasaki, M., Ito, H. & Kikutani, T. 2003. Development of stereocomplex crystal of polylactide in high-speed melt spinning and subsequent drawing and annealing processes. Journal of Macromolecular Science – Physics 42, pp. 403-420.

Teijin. 2009. [WWW] News Release. Teijin expands hygrothermal resistance of Biofront™ bioplastic upgraded version now offers high durability comparable to PET. Available at: http:www.teijin.co.jp/English/news/2009/ebd090708.html.

Turner II, J.F., Riga, A., O'Connor, A., Zhang, J. & Collis, J. 2004. Characterization of drawn and undrawn poly-L-lactide films by differential scanning calorimetry. Journal of Thermal Analysis and Calorimetry 75, pp. 257-268.

Tsuji, H. 2000. In vitro hydrolysis of blends from enantiomeric poly(lactide)s Part 1. Well-stereo-complexed blend and non-blended films. Polymer 41, pp. 3621-3630.

Tsuji, H. 2005. Poly(lactide) stereocomplexes: formation, structure, properties, degredation, and applications. Macromolecular Bioscience 5, pp. 569-597.

Tsuji, H., Hyon, S.-H. & Ikada, Y. 1991. Stereocomplex formation between enantiomeric poly(lactic acid)s. 3. Calorimetric studies on blend film cast from dilute solution. Macromolecules 24, pp. 5651-5656.

Tsuji, H., Ikada, Y., Hyon, S.-H., Kimura, Y. & Kitao, T. 1994. Stereocomplex formation between enantiomeric poly(lactic acid). VIII. Complex fibers spun from mixed solution of poly(D-lactic acid) and poly(L-lactic acid). Journal of Applied Polymer Science 51, pp. 337-344.

Tsuji, H., Nakano, M., Hashimoto, M. Takashima, K., Katsura, S. & Mizuno, A. 2006. Electrospinning of poly(lactic acid) stereocomplex nanofibers. Biomacromolecules 7, pp. 3316-3320.

Tsurumi, T. 1994. Solution Spinning. In: Nakajima, T., Kajiwara, K. & McIntyre J. E. (ed.). Advanced fiber spinning technology. Cambridge, UK, Woodhead Publishing Limited. pp. 65-104.

Van de Witte, P., Esselbrugge, H., Peters, A.M.P., Dijkstra, P.J., Feijen, J., Groenewegen, R.J.J., Smid, J., Olijslager, J., Schakenraad, J.M., Eenink, M.J.D. & Sam, A.P. 1993. Formation of porous membranes for drug delivery systems. Journal of Controlled Release 24, pp. 61-78.

Veiranto, M., Törmälä, P. & Suokas, E. 2002. In vitro mechanical and drug release properties of bioabsorbalbe ciprofloxacin containing and neat self-reinforced P(L/DL)LA 70/30 fixation screws. Journal of Materials Science: Materials in Medicine 13, pp. 1259-1263.

Vert, M., Li, S. M., Spenlehauer, G. & Guerin, P. 1992. Bioresorbability and biocompatibility of aliphatic polyesters. Journal of Materials Science: Materials in Medicine 3, pp. 432-446.

Vink, T.H., Rábago, K. R., Glassner, D.A. & Gruber, P.R. 2003. Applications of life cycle assessment to NatureWorks™ polylactide (PLA) production. Polymer Degradation and Stability 80, pp. 403-419.

Vink, T.H., Rábago, K.R., Glassner, D.A., Springs, B., O'Connor, R.P., Kolstad, J. & Gruber, P.R. 2004. The sustainability of Nature Works™ polylactide polymers and Ingeo™ polylactide fibers: an update of the future. Macromolecular Bioscience 4, pp. 551-564.

Wang, X., Zhang, K., Zhu, M., Yu, H., Zhou, Z., Chen, Y. & Hsiao, B. S. 2008 Continuous polymer nanofiber yarns prepared by self-bundling electrospinning method. Polymer 49, pp. 2755-2761.

Wang, Y., Steinhoff, B., Brinkmann, C. & Alig, I. 2008. In-line monitoring of the thermal degradation of poly(l-lactic acid) during melts extrusion by UV-vis spectroscopy. Polymer 49, pp. 1257 -1265.

Weiler, W. & Gogolewski, S. 1996. Enhancement of the mechanical properties of polylactides by solid-state extrusion I. Poly(D-lactide). Biomaterials 17, pp. 529-535.

Wilkes, A.G. 2001. The viscose process. In: Woodings, C. (ed.). Regenerated cellulose fibres. Cambridge, UK, Woodhead Publishing Limited. pp. 37-61.

Yamanaka, K. 1999 Lactron – a biodegradable fiber, its development and applications. Chemical Fibers International 49, p. 501.

Yang, F., Xu, C.Y., Kotaki, M., Wang, S. & Ramakrishna, S. 2004 Characterization of neural stem cells on electrospun poly(L-lactic acid) nanofibrous scaffold. Journal of Biomaterials Science, Polymer Edition 15, pp. 1483-1497.

Yang, F., Murugan, R., Wang, S. & Ramakrishna, S. 2005. Electrospinning of nano/micro scale poly(L-lactic acid) aligned fibers and their potential in neural tissue engineering. Biomaterials 26, pp. 2603-2610.

You, Y., Min, B.-M., Lee, S.J., Lee, T.S. & Park, W.H. 2005. *In vitro* degradation behavior of electrospun polyglycolide, polylactide, and poly(lactide-*co*-glycolide). Journal of Applied Polymers Science 95, pp. 193-200.

Yuan, X., Mak, A.F.T., Kwok, K.W., Yung, B.K.O. & Yao, K. 2001. Characterization of Poly(L-lactic acid) fibers produced by melt spinning. Journal of Applied Polymer Science 81, pp. 251-260.

Zhmayev, E., Zhou, H. & Joo, Y.L. 2008 Modeling of non-isothermal polymer jets in melt electrospinning. Journal of Non-Newtonian Fluid Mechanics 153, pp. 95-108.

Zhou, H., Green, T.B. & Joo, Y.L. 2006. The thermal effects on electrospinning of polylactic acid melts. Polymer 47, pp. 7497-7505.

Zilberman, M., Schwade, N.D. & Eberhart, R. C. 2004. Protein-loaded bioresorbable fibers and expandable stents: mechanical properties and protein release. Journal of Biomedical Materials Research Part B Applied Biomaterials 69, pp. 1-10.

SUMMARIES OF PAPERS

Paper I, "Solubility and Phase Separation of Poly(L,D-lactide) Copolymers", studies the solubility of polylactide stereo copolymers having different L to D ratios and the phase separation ability of the polymer solutions. The solubility trials were done using different organic solvent, and the phase separation ability was tested using cloud-point titration using different organic non-solvents. The solubility of copolymers was dependent on the L to D ratio; P(L/D)LA 50/50 was the most soluble polymer and P(L/D)LA 96/4 was the least soluble polymer. The cloud point titration results showed that *n*-hexane was the most efficient precipitant from the analyzed non-solvents. Methanol and ethanol showed quite similar precipitation properties, whereas the isopropyl alcohol was the least efficient precipitant from the analyzed non-solvents. Furthermore, the L to D ratio had effect on the phase separation rate. The precipitation happened most rapidly with the P(L/D)LA 96/4 solution because the analyzed non-solvents were far from the solubility gap of the P(L/D)LA 96/4 polymer.

Paper II, "Effect of Process Parameters on Properties of Wet-Spun Poly(L,D-lactide) Copolymer Multifilament Fibers", studies the effect of the spin draw ratio and the constitution of the spin bath on the mechanical and the *in vitro* degradation properties. According to previous Paper I methanol and ethanol were chosen for the spin baths and P(L/D)LA 96/4 and P(L/DL)LA 70/30 for the filament polymers. The diameter and the mechanical properties were dependent on the spin draw ratio. The spin bath had minor effect on the filament properties. Because methanol is a smaller molecule than ethanol, it caused slightly faster precipitation. The filaments precipitated in the swollen state, and thus the methanol coagulated P(L/D)LA 96/4 filaments were slightly thicker than the ethanol coagulated filaments. The degree of crystallinity of the wet-spun filaments was lower compared to the original polymer granulates. The P(L/D)LA 96/4 filaments were semi-crystalline and the P(L/DL)LA 70/30 filaments were totally amorphous. Thus, the *in vitro* degradation rate of the P(L/DL)LA 70/30 was faster than that of the P(L/D)LA 96/4 filament.

Paper III, "Effect of Hot Drawing on Properties of Wet-Spun Poly(L,D-lactide) Copolymer Multifilament Fibers", studies the effect of hot drawing on the mechanical

and the *in vitro* degradation properties. Hot drawing increased the mechanical strength of the P(L/D)LA 96/4 filaments compared to the spin-drawn filaments. Furthermore, hot drawing increased the degree of crystallinity of the P(L/D)LA 96/4 filaments. The hot-drawn P(L/DL)LA 70/30 filaments were practically amorphous. The *in vitro* degradation rate of the hot-drawn filaments was slower compared to the as-spun filaments due the increased orientation of molecular chain and the increased crystallinity.

Paper IV, "Effect of Protein-Loading on Properties of Wet-Spun Poly(L,D-lactide) Multifilament Fibers", studies the effect of BSA-loading on the mechanical and *in vitro* properties. The protein-loaded filaments were fabricated from protein-polymer emulsion made by a probe sonicator. The filaments had a distinct porous cross-section structure according to the SEM-images. The large pores were caused from the sonication, whereas the small pores were caused the interaction of solvent and non-solvent in the spin bath. The protein-loading decreased significantly the mechanical properties of the filaments. The release rate of BSA was very slow due to the big size of the BSA molecule and the slow degradation of copolymers.

Paper I

Marja Rissanen, Arja Puolakka, Pertti Nousiainen, Minna Kellomäki, Ville Ellä

Solubility and Phase Separation of Poly(L,D-lactide) Copolymers

Journal of Applied Polymer Science, 110 (2008) pp. 2399-2404

Paper II

Marja Rissanen, Arja Puolakka, Terttu Hukka, Ville Ellä, Pertti Nousiainen, Minna Kellomäki

Effect of Process Parameters on Properties of Wet-Spun Poly(L,D-lactide) Copolymer Multifilament Fibers

Journal of Applied Polymer Science, 113 (2009) pp. 2683-2692

Paper III

Marja Rissanen, Arja Puolakka, Terttu Hukka, Ville Ellä, Minna Kellomäki, Pertti Nousiainen

Effect of Hot Drawing on Properties of Wet-Spun Poly(L,D-Lactide) Copolymer Multifilament Fibers

Journal of Applied Polymer Science, 115 (2010) pp. 608-615

Paper IV

Marja Rissanen, Arja Puolakka, Niina Ahola, Aaron Tonry, Yury Rochev, Minna Kellomäki, Pertti Nousiainen

Effect of Protein-Loading on Properties of Wet-Spun Poly(L,D-lactide) Multifilament Fibers

Journal of Applied Polymer Science, 116 (2010) pp. 2174-2180